End of the Kiaman Superchron in the Permian of SW England: Magnetostratigraphy of the Aylesbeare Mudstone and Exeter groups.

Mark W. Hounslow*[1], Gregg McIntosh[2], Richard A. Edwards[3], Deryck J. C. Laming[4], Vassil Karloukovski[1]

[1]*Lancaster Environment Centre, Lancaster University, Lancaster, LA1 4YW, U.K.*
[2] *School of Human and Life Science, Canterbury Christchurch University, Canterbury, UK.*
[3]*Hawkridge, Thorverton, Devon, EX5 5JL, U.K (formerly British Geological Survey, Exeter, UK)*
[4]*Herrington Geoscience and David Roche GeoConsulting, Renslade House, Bonhay Road, Exeter EX4 3AY, Devon, UK.*

*Corresponding author (e-mail: m.hounslow@lancaster.ac.uk :Tel:+ 44 (0) 1524 510238

Number of: words of text (=8223), words in captions (=1140), references (=103), Tables (=1) and figures (=11)

Abbreviated title (< 40 characters) : **Kiaman Superchron, SW England**

Keywords: **Magnetostratigraphy, Permian, Triassic, Kiaman Superchron, Rotliegend**

Abstract: The chronology of Permian strata in SW England is fragmentary and largely based on radiometric dating of associated volcanic units. Magnetostratigraphy from the ~2 km of sediments in the Exeter and Aylesbeare Mudstone groups was undertaken to define a detailed chronology, using the end of the Kiaman superchron, and the overlying reverse and normal polarity in the Middle and Upper Permian as age constraints. The palaeomagnetic directions are consistent with other European Permian palaeopoles, with data passing fold and reversal tests. The end of the Kiaman superchron (in the Wordian) occurs in the uppermost part of the Exeter Group. The overlying Aylesbeare Mudstone Group is early Capitanian to latest Wuchiapingian in age. The Changhsingian and most of the Lower Triassic is absent. Magnetostratigraphic comparison with the Southern Permian Basin shows that the Exeter and Aylesbeare Mudstone groups are closely comparable in age to the Havel and Elbe Subgroups of the Rotleigend II succession. The Altmark unconformities in these successions appear similar in age as the sequence boundaries in SW England, indicating both may be climate controlled. Clasts in the Exeter Group, from unroofing of the Dartmoor granite, first occurred at a minimum of ~8 Ma after formation of the granite.

Supplementary material: Additional magnetic fabric and palaeomagnetic data is available at: hhttp://www.geolsoc.org.uk/SUP000

Permian and Triassic successions in southern and SW England were produced following the Variscan orogeny and occur in a number of interconnected, sag and fault-bounded basins, the largest being the Wessex Basin, and various sub-basins that form the Channel Approaches Basin. Some basins contain up to 8 km of post-Variscan red-bed fill (Harvey *et al.* 1994; Hamblin *et al*. 1992; Butler 1998; McKie & Williams 2009; Fig. 1). The Wessex Basin formed on Rheno-Hercynian basement (Variscan), between the Northern Variscan Front and the Lizard-Rhenish Suture. The sub-basins of the Western Approaches Basin formed on Saxo-Thuringian (Variscan) and Rheno-Hercynian basement (McCann *et al*. 2006; Strachan *et al.* 2014). As such, these basins may share similar tectonic and stratigraphic histories with similarly situated basins in France and Germany such the Saar-Nahe and Saale basins in Germany (Roscher & Schneider 2006; McCann *et al*. 2006.). However, our tectono-stratigraphic understanding of the UK basins is poorly integrated into the framework of European Permian basin evolution. These intramontane basins often lack the distinctive late Permian carbonate-evaporite, Zechstein successions, common in basins (e.g. Southern Permian Basin) north of the Variscan front, and lack the early Permian faunas of the southern Variscan basins (Roscher & Schneider 2006; McCann *et al*. 2006).

The onshore Permian-Triassic successions in the western parts of the Wessex Basin and the Credition Trough, outcrop as the Exeter, Aylesbeare Mudstone and Sherwood Sandstone groups (Figs. 1 & 2). The coastal outcrops form part of the Jurassic Coast World Heritage Site (Barton *et al.* 2011). The work of the British Geological Survey, related to the re-mapping of the Exeter area (Edwards *et al*. 1997), generated a better regional understanding of the Permian Exeter Group (Gp). The oldest successions outcropping in the Crediton Trough (and Torbay area) may extend into the latest Carboniferous (Edwards *et al*. 1997; Leveridge *et al*. 2003). The units below the base of the Whipton Formation (Fm) in the Exeter and Crediton Trough area contain a variety of basaltic and lamprophyric lavas and intrusions, whose Ar-Ar and K-Ar ages (291-282 Ma) are older than the more tightly constrained Rb-Sr, U-Pb and Ar-Ar ages (at 280 Ma) for the formation of the Dartmoor Granite (Scrivener 2006). These volcanic and igneous units are coeval with widespread volcanic activity throughout Europe during the latest Carboniferous to early Permian (Timmerman 2004). The isostatic uplift and regional denudation coeval with, and following, Dartmoor Granite emplacement, was probably responsible for a major unconformity (Edwards *et al*. 1997) separating the Whipton Fm from the older units (Fig. 2).

Miospores from the Whipton Fm around Exeter, and younger units equivalent to the Alphington and Heavitree Breccia formations, demonstrate similarities to assemblages from the Russian Kazanian and Tatarian regional stages (Warrington & Scrivener 1990; Edwards *et al*. 1999). Consequently, the barren overlying Aylesbeare Mudstone Gp has been assigned to the Lower Triassic in some subsequent studies (Newell 2001; Benton *et al*. 2002). Since the Aylesbeare Mudstone Gp is widespread in the Wessex Basin and the western approaches (Hamblin *et al*. 1992; Butler 1998; Evans 1990; Barton *et al.* 2011), a Lower Triassic mudstone-dominated lacustrine unit creates a major palaeogeographic problem. That is, southerly-derived clasts in the Lower Triassic units, in central and Northern Britain, could not have been sourced through the Wessex Basin, from the Armorican supply areas to the south, as has been widely concluded for over 100 years (Ussher 1876; Thomas 1909; Wills 1970; McKie & Williams 2009; Morton *et al.* 2013).

To resolve this problem, and constrain in detail the age of the Permian successions, we use magnetostratigraphy as a dating tool. The Kiaman (reverse polarity) superchron (KRPS) extends from the mid Carboniferous to the mid Permian, but had ended by the early Wordian (mid Guadalupian), after which reverse and normal polarity intervals (here called the Illawarra Superchron) occur during the remainder of the mid and late Permian, extending into the Triassic (Steiner 2006; Hounslow submitted). We demonstrate for the first time in the UK, the stratigraphic position of the end of the KRPS, and also the polarity pattern through the upper part of these successions (below the Budleigh Salterton Pebble Beds Fm). Our data allows a new understanding of the precise age of these units, which suggests a new relationship to the better-studied successions in the Southern Permian Basin.

Geology and Lithostratigraphy

Excellent exposures of the Exeter and Aylesbeare Mudstone groups occur in a series of cliff and foreshore exposures between Torbay and Budleigh Salterton (Fig. 1). These sediments have maximum burial temperatures of ca. 80±5^{o}C attained during the early Cretaceous, with estimated maximum burial depths of 2 to 2.5 km (Carter *et al.* 1995). Faulting and folding structures in the Wessex Basin are a response to basin inversion, produced by N-S compression, along mostly E-W trending faults, many of which were former extensional structures. The basin inversion took place during the late Cretaceous and early Tertiary (Underhill & Stoneley 1998).

Exeter Group

The Exeter Group is predominantly the deposits of a number of alluvial fans, with aeolian dune sandstones dominating in the Dawlish Sandstone Fm, and in some units in the Torbay Breccia Fm (Fig. 2). The coastal successions in Torbay are separated from those north of Oddicombe (Fig. 1) by the Torquay-Babbacombe promontory which was a palaeogeographic feature in the Permian (Laming 1966). Mapping work indicates the Torbay Breccia Fm (Leveridge *et al*. 2003), can be divided into a number of separate breccias units with differing clast contents (unpublished work of DJCL). The Watcombe Fm which is an on-lapping mudstone-rich breccia unit, which north of the Torquay-Babbacombe promontory is unconformably overlain by the Oddicombe Breccia Fm (and the equivalent Paignton breccias south of this). On the coastal outcrops the Watcombe Fm has a 9-20^{o} dip-discordance with the overlying Oddicombe Breccia (9^{o} at Whitsand Bay and 20^{o} at Oddicombe Cove; Figs. 1, 3d; Laming 1982). The lower parts of the Torbay Breccia Fm (Roundham Head breccias, with clasts derived from SW) are generally poor in volcanic clasts (Laming 1982) like the oldest unit (the Cadbury Breccia Fm; Edwards & Scrivener 1999) in the Crediton Trough, and by inference may have similar ages, prior to the early Permian basaltic volcanism.

The various breccia units below the Dawlish Sandstone Fm are largely distinguished by their clast contents. These contain a variety of lithologies (limestone, sandstone, vein quartz, quartzite and slate) from various Variscan basement units, together with a variety of volcanic rock fragments associated with the granite and its former or earlier extrusives (Laming 1982; Selwood *et al*. 1984; Edwards & Scrivener 1999). The Watcombe and Whipton formations consist of fine-grained sandy or muddy breccia with clasts of slate and sandstone with occasional porphyry. They contain irregularly interbedded sandstone and mudstone units (Ussher 1913), which dominate the Whipton Fm around Exeter (Edwards & Scrivener 1999). The Oddicombe Breccia Fm (Fig. 2) is rich in locally derived limestone fragments, which typically displays fining-up sequences (into poorly sorted sandstones or fine-breccias; Benton *et al*. 2002) several metres thick, well displayed at Maidencombe Cove and Bundle Head (Figs. 1, 4). The Alphington Breccia Fm is likewise rich in locally derived shale and sandstone fragments, and hornfelised shale from the underlying Variscan basement (Edwards *et al*. 1997). The Teignmouth and Heavitree formations are distinctive in containing common clasts of pink and white perthitic feldspar (murchisonite), which Dangerfield & Hawkes (1969) interpreted as feldspar megacrysts from the roof zone of the Dartmoor granite; the supply of which probably indicates synchronous

unroofing into adjacent alluvial fan successions. The older Alphington and Oddicombe Breccia formations lack the murchisonite clasts (Selwood *et al*. 1984; Edwards & Scrivener 1999).

All the breccia units tend to be poorly sorted, and may locally contain a high proportion of mud or sand. The fining-up successions in the Teignmouth Breccia Fm tend to be smaller scale (< 1 m thickness) and typically display poor lateral organisation. Breccias in the upper-part of this formation have interbedded aeolian sandstone units, well displayed in the Coryton Cove area (8 on Fig. 1; Fig. 4); which is a transitional part of this formation into the overlying Dawlish Sandstone Fm. The estimated thicknesses of the Oddicombe and Teignmouth Breccia formations vary widely between different authors, because of faulting, variable bedding dips and probably significant palaeotopography on the Variscan basement. The thicknesses of Selwood *et al*. (1984) are minimum thickness estimates, whereas Laming (1969; 1982) and this work suggest greater thicknesses at the upper limits indicated in Fig. 2.

The aeolian dune systems that dominate deposition in the Dawlish Sandstone Fm (Newell 2001), also display interbedded fluvial sandstone and breccia units. Around Exeter and further north in the Crediton Trough, the Dawlish Sandstone Fm onlaps onto older units, to rest on Variscan basement. The overlying Exe Breccia Fm is divisible into a lower porphyry-bearing unit (the Kenton Mbr), typical of most of the outcrop on the west of the Exe Estuary, and an overlying quartzite- and mudstone-bearing breccia (the Langstone Mbr). This upper member is well exposed at Langstone Rock (6 on Fig. 1) which in the upper part is dominated by poorly sorted sandstones and sandy siltstones (Gallois 2014; Fig. 4). The thickness of the Exe Breccia is uncertain, due to faulting along the Exe Estuary; 85 m was suggested by Selwood *et al*. (1984), but up to ~50 m is more likely (Laming & Roche 2013). The uppermost part of the Langstone Mbr at Lympstone and Sowden Lane (3 on Fig. 1) displays both well-developed shallow fluvial channels and aeolian sandstone units, and is gradational into the mudstones and siltstones forming the base of the Aylesbeare Mudstone Gp (Gallois 2014; Fig. 4). Around Exeter and in the Crediton Trough the Aylesbeare Mudstone Gp is unconformable on the Dawlish Sandstone Fm, also onlapping onto older units (Edwards *et al*. 1997; Edwards & Scrivener 1999).

Aylesbeare Mudstone Group

The Exmouth Mudstone and Sandstone Fm is a lacustrine, red-brown mudstone-dominated unit, with interbedded fine to medium-grained fluvial and lacustrine sandstone units (thicker beds

167 labelled as Beds A to J by Selwood *et al*. 1984). These are most prominent towards the upper
168 part of the formation, where the term Straight Point Sandstone Mbr is introduced for these
169 persistent sandstone beds (i.e. beds I and J of Selwood *et al*. 1984). This member is mapped
170 between the coast and Aylesbeare, north of which the Aylesbeare Mudstone Gp is not sub-
171 divided (Edwards & Scrivener 1999). The upper few metres of the Straight Point Sandstone Mbr
172 at outcrop has patchily developed, immature, nodular and sheet-like groundwater calcretes,
173 locally with rhizoconcretions (Fig. 3B). The base of the overlying Littleham Mudstone Fm is
174 taken at the base of the porphyry and murchisonite bearing breccia unit (Ormerod-Wareing
175 1875), which locally erosively overlies this calcrete-bearing sandstone (Fig. 3C), and grades into
176 overlying interbedded sandstone, siltstone and mudstone beds in the basal parts of the Littleham
177 Mudstone Fm, west of the Littleham Cove fault (Fig. 5).
178
179 The Littleham Mudstone Fm is well-exposed in the cliffs between Littleham Cove and Budleigh
180 Salterton, but is locally disrupted by faulting in the lower part and landslips in the cliff. The
181 complete succession in the cliffs was determined by using a montage of photographs taken from
182 offshore, which shows the full succession is divided by a number of prominent green mudstone,
183 thin sandstone and siltstone beds (Fig. 5). The succession in the cliffs can be divided into three
184 units, a lower unit (Division A) east of the Littleham Cove fault with a few green mudstone beds,
185 a middle unit (Division B) with relatively common sandstone and siltstone beds, and an upper
186 unit (Division C) with more frequent green mudstone beds and some impersistant sandstones.
187 The true thickness of the Littleham Mudstone Fm, in these outcrops, cannot be determined
188 because of the uncertain displacement on the Littleham Cove fault. However, the measured
189 cumulative thickness east and west of the fault (216 m), is similar to the ~205 m and 230 m
190 measured in the Blackhill and Withycombe Rayleigh boreholes respectively (Bateson & Johnson
191 1992; Fig. 1), so the cliff outcrops probably represent most of the Littleham Mudstone Fm. In the
192 Venn Ottery borehole (Fig. 1) the Littleham Mudstone Fm contains pods and veins of gypsum,
193 and thin interbedded aeolian sandstones (Bateson & Johnson 1992; Edwards & Scrivener 1999;
194 N.S Jones pers comm to RAE). A substantial unconformity separates the Littleham Mudstone Fm
195 from the overlying Budleigh Salterton Pebble Beds Fm, shown by the dramatic lithology change,
196 and the sharp and irregular boundary (Fig. 3A) with some authors suggesting a small bedding dip
197 difference (Irving, 1888). Gallois (2014) has suggested this contact is conformable.

Regional relationships

Broadly the Permian units in the study area can be divided into 5 genetic sequences (Pm1 to Pm5), bounded by a hiatus or unconformity (Fig. 2). The upper three of these are all characterised by basal breccias units (low stand deposits), with conformable transitions into overlying finer-grained upper parts. The relationships of the successions in Torbay to those in the Crediton Trough area is less certain. It is probable that the earliest parts of the Torbay Breccia Fm is timing-related to the Cadbury Breccia Fm in the Crediton Trough (sequence Pm1), since both units are very poor in igneous clasts (Edwards *et al.* 1997). These five sequences may relate to the four sequences (A to D) seen in the Plymouth Bay Basin (Harvey *et al.* 1994). Their oldest megasequence A likely relates to Pm1 and megasequence B to Pm2, since it is capped by an inferred volcanic unit. Megasequence C likely relates to Pm3, and is marked by a change in orientation of the Plymouth Bay Basin depocentres. Divergent bedding dips between units under and overlying the Watcombe Fm (Pm2), suggest that the most important extensional event (Leveridge *et al*. 2003; Laming 1982) is at the Pm2-Pm3 boundary, consistent with depocentre orientation change in the Plymouth bay basin. Megasequence D is probably equivalent to Pm4 and Pm5, since the Pm4-Pm5 boundary is subtle to detect in the field.

The continuity of these units to the east in the central parts of the Wessex Basin is uncertain. Henson (1972) suggested, based on geophysics, that the breccia units thin to the east, so eastwards the breccias may pass into the mudstone dominated units, equated with the Aylesbeare Mudstone Gp in the central parts of the Wessex Basin, which are up to ~1.5 km thick (Butler 1998; Hamblin *et al*. 1992). However, Henson's data failed to detect the faults, along the Exe Estuary, so the interpretation may be flawed. In the Western Approaches basins 1 km or more of anhydritic mudstones and sandstones underlie the equivalent of the Sherwood Sandstone Gp (Evans 1990). These locally rest on a Permian volcanic sequence, presumably of a similar age to the early Permian Exeter Volcanic Rocks (Chapman 1989; Fig. 2).

Palaeomagnetic sampling

Almost the entire succession of the Aylesbeare Mudstone Gp is exposed in the sea-cliffs between Budleigh Salterton and Exmouth. Only the mid and upper parts of the Exe Breccia could be sampled at Lympstone (location 3 on Fig.1) and Langstone Rock (6 on Fig. 1; see Supplementary data for details). Outcrops in the lower parts of the Exe Breccia Fm (Kenton Mbr), were all too coarse-grained for palaeomagnetic sampling. Most of the Dawlish Sandstone and Teignmouth

Breccia are well exposed between Langstone Rock and Teignmouth, adjacent to the main London-Penzance railway-line (Ussher 1913; Selwood *et al*. 1984), but large parts are inaccessible due to rail-safety restrictions. The Dawlish Sandstone Fm was sampled in quarries near Exeter (4 and 5 on Fig. 1; Fig. 4). The uppermost part of the Teignmouth Breccia was available for sampling in the Coryton Cove and Dawlish Station sections (7 and 8 on Figs. 1, 4). Reconnaissance sampling of the Oddicombe and Watcombe Breccias was undertaken. For the most part, these units are fully exposed in sea-cliffs and foreshore exposes between Teignmouth and Oddicombe (Fig. 4). The Knowle Sandstone Fm was sampled at west Sandford (Edwards *et al.* 1997).

Samples from these units were collected using mostly hand samples, oriented with a compass. In total some 153 samples were collected from 13 sites (see Supplementary data), largely focussed on reddened lithologies. Cubic specimens were cut from the hand samples using a circular saw. Some samples from sandstone units in the Dawlish Sandstone and Exe and Teignmouth Breccias were poorly consolidated, and impregnated in the laboratory with a 2:1 mix of sodium silicate and water (Kostadinova *et al*. 2004) to consolidate them prior specimen preparation.

Laboratory Methodology

Measurements of Natural Remanent Magnetisation (NRM) were made using a CCL 3-axis cryogenic magnetometer (noise level ~0.002 mA/m), using multiple specimen positions, from which the magnetisation variance was determined. The magnetometer is not housed in a controlled space which cancels the earth's magnetic field. Instead specimens were housed in Mu-metal boxes with an ambient magnetic field <10 nT at all times, other than when being measured or demagnetised. Generally, 1 to 3 specimens from each sample were treated to stepwise thermal demagnetisation, using a Magnetic Measurements Ltd thermal demagnetiser, in 50-40°C steps up to 700°C. Low frequency magnetic susceptibility (K_{lf}) was monitored after heating stages, measured using a Bartington MS2B sensor. Specimens from the Bishops Court Quarry gave poor quality results and sister specimens were partly treated with a combination of thermal and alternating field (AF) demagnetisation, the latter conducted using a Molspin tumbling AF demagnetiser. In total 166 and 78 paleomagnetic specimens were demagnetised from the Aylesbeare Mudstone and Exeter groups respectively. The bedding dips in the Aylesbeare Mudstone Gp are 5-10^{o} in an easterly direction, so a fold test was not possible. However, in the Exeter Gp dips are more variable and up to 40^{o}, so a fold-test was possible.

Characteristic remanent magnetisation (ChRM) directions were isolated using principal component-based statistical procedures as implemented in LINEFIND, which uses the measurement variance along with rigorous statistical procedures for identifying linear and planar structure in the demagnetisation data (Kent *et al*. 1983). Both linear trajectory fits and great circle (remagnetisation circle) data were used in defining the paleomagnetic behaviour, guided by objective and qualitative selection of the excess standard deviation parameter (ρ), which governs how closely the model variance, used for analysis, matches the data measurement variance (Kent *et al*. 1983). The PMAGTOOL software (available at https:\\www.lancs.ac.uk\staff\hounslow\default.htm) was used for the analysis of mean directions and virtual geomagnetic poles.

Progressive isothermal remanent magnetisation (IRM) up to 1T is most and 4 T is some was applied to a representative sub-set of specimens, to investigate the magnetic mineralogy. Back field demagnetisation was also used on some specimens. This used an ASC Scientific IM-30 impulse magnetiser and a Molspin pulse magnetiser. The IRM was measured using a Molspin spinner magnetometer. Thermal demagnetisation of a three component IRM was used to investigate the unblocking temperatures (Lowrie 1990). A small set of specimens were measured for magnetic hysteresis (maximum field 0.9 T) and thermomagnetic curves (maximum field 300 mT, in air using a Magnetic measurements variable field translation balance, MMVFTB). Selected thin sections were investigated to assess the petrography of the Fe-oxides. The anisotropy of magnetic susceptibility (AMS), of selected specimens, was measured using an Agico KLY3S Kappameter, to assess the preservation of the detrital sedimentary fabric (Løvlie & Torsvik 1984; Tarling & Hrouda 1993), and to assess if fabrics had been modified by the weak tectonism.

Magnetic Mineralogy

Changes in the NRM intensity and K_{lf} of specimens are broadly related to:

a) The amount of silt and clay, with those samples having larger amounts of silt and clay generally having larger NRM intensity and K_{lf}. For example, aeolian sandstones such as those in the Dawlish Sandstone Fm, have significantly lower NRM intensity and K_{lf} (Fig. 5, see Supplementary data). In the Aylesbeare Mudstone Gp red mudstones possess average

293 NRM intensity and K_{lf} of 5.0 mA/m and 20.0 x10^{-6} SI respectively, compared to means of 1.8
294 mA/m and 7.2 x10^{-6} SI in the red sandstone beds.
295 b) Reddened and non-reddened samples of the same lithology often possesses dramatically
296 different NRM intensity and K_{lf}; with the non-reddened samples typically having lower
297 values. For example grey, green and white sandstones in the Aylesbeare Mudstone Gp have
298 mean NRM intensity and K_{lf} of 0.9 mA/m and 4.4 x10^{-6} SI respectively.
299 c) The average NRM intensity and K_{lf} shows progressively larger values into the Oddicombe
300 Breccia and Watcombe formations (see supplementary data). This may relate to a progressive
301 increase in volcanic-derived detritus (and iron oxide content) in the older units, which is
302 shown by the Cs content (Merefield *et al*. 1981).
303
304 Specimens analysed do not saturate in IRM fields up to 4 T (Fig. 6A, C), indicating that canted
305 antiferrimagnetic minerals (haematite or goethite) are important magnetic minerals in these
306 specimens. Durrance *et al*. (1978) also detected haematite as the main Fe-oxide in the Littleham
307 Mudstone Fm, with the addition of significant amounts of superparamagnetic haematite.
308 Thermomagnetic curves were nearly reversible and exhibited Curie temperatures of 657-669°C,
309 and thermal demagnetisation of the IRM, shows that specimens display blocking temperatures up
310 to 650-700°C (Fig. 6). Coercivity of remanence (Bcr) ranged between 320 and 710 mT, all
311 suggesting predominant haematite (Frank & Nowaczyk 2008). Although the IRM does not
312 approach saturation by 4 T (Fig. 6B), there is no clear evidence for goethite, since we have high
313 SIRM/ K_{lf} values, and no well-defined Neel temperature for goethite. Percent IRM acquisition
314 below 100 mT (%IRM_{100mT}) is mostly 5%-10% of the 1T IRM, for reddened lithologies. Only in
315 aeolian sandstone units in the Dawlish Sandstone Fm, and grey or red mottled green/grey
316 lithologies does the %IRM_{100mT} rise above 10% to ca. 50% at maximum (Fig. 6A,C,E). Data
317 from synthetic mixtures (Frank & Nowaczyk 2008) suggest such %IRM_{100mT} values indicate a
318 magnetite contribution to the iron oxide load of ca. 0.05% (for red lithologies) to a maximum of
319 ca. 1% for aeolian samples DS16 and DS100 (Fig. 6E). In specimens DS16, (from Dawlish
320 Sandstone Fm aeolian sandstones; Fig. 6F) and L3 (grey sandstone, Littleham Mudstones Fm;
321 Fig. 6B) the 100 mT IRM demagnetises by 450°C- 550°C, which could suggest an oxidized, or
322 Ti-poor magnetite (Fig. 6F). The >300 mT coercivity component in specimen DS16 has a
323 blocking temperature of ~550°C, probably due to a pigment-dominated haematite remanence
324 (Turner 1979) in this sample.
325

Petrography indicates, like other red-beds, that the haematite is present as two phases, firstly sub-micron haematite (pigmentary haematite), which coats pore perimeters and is often internal to some rock clasts; secondly as larger specular haematite particles, most obvious as detrital opaque grains (Turner 1979; Fig. 3E, F). The pore-lining pigmentary haematite is multiphase in origin, since it both coats feldspar overgrowths, and to a lesser extent, coats the grains prior to the overgrowths (observed in Dawlish Sandstone Fm only). Compaction related pressure solution at some grain contacts, shows greater amounts of pigment coating the pores, and lesser amounts between the grain contacts, demonstrating both pre and post-compaction pigmentary haematite formation, with probably the bulk of the pigment produced post compaction. Some of the pigmentary haematite may have formed pre-deposition, since it is widely dispersed within a variety of siltstone and phyllite clasts.

The specular haematite is dominated by detrital opaques, which are either present as haematite dominated particles, or compound particles in-part composed of other silicate minerals. The compound particles are occasional haematised clastic rock fragments (intraformational?) but most are of uncertain origin (Fig. 3E). These two types of specularite grains vary in abundance from about 1% to trace amounts. Larger amounts of detrital opaques tend to occur in samples that are finer-grained or less well sorted, and lesser amounts in the well-sorted aeolian sandstones.

Magnetic Fabric

The anisotropy of magnetic susceptibility (AMS) overall shows a primary depositional magnetic fabric, characterised by vertical-to-bedding K_{min} directions (Figs. 7 a-d) and largely oblate ($T > 0$) fabrics (Figs. 7 e - h). The mudstones have the stronger AMS (greater P values) and are always oblate. The sandstones within the Aylesbeare Mudstone Gp and the various breccia units show more variable AMS fabrics ranging into the prolate fields ($T < 0$), especially so for some sandstones from the breccia units (Fig. 7e, h). This may relate to the more poorly sorted, probably more chaotically deposited grains in the breccia units (possibly related to mudflow deposition, *cf.* Park *et al.* 2013). K_{max} axis trends (Figs. 7i) for specimens from the breccia units (Fig. 7l) show both N-S trends and ENE-WSW trends similar to the clast imbrication directions (typically between easterly and northerly directions) of Laming (1982) and Selwood *et al.* (1984). This demonstrates the K_{max} directions parallel the fluvial transport directions. The N-S directed K_{max} axes trends are common near the Babbacombe-Torquay promontory and in the Teignmouth Breccia Fm. Similar easterly and northeasterly K_{max} axes trends are present in the

Exmouth Sandstones and Mudstones, whereas those in the Littleham Mudstone Fm are more variable.

Specimens from aeolian sandstones (from the Dawlish Sandstone Fm and upper part of the Teignmouth Breccia Fm) show a larger proportion of prolate fabrics (T <0) with many more K_{min} axes deviating from vertical (Figs. 7c, g). This may be partly caused by the AMS in these specimens being closer to the sensitivity limits of the KLY3S. However, it is also a reflection of the rolling grain transport on the leeward slip-faces of the aeolian dunes (Ellwood & Howard 1981), producing a grain long-axis orientation transverse to the average wind direction (Schwarzacher 1951), which was to the NW to NNW (Laming 1982; Newell 2001). This is clearly shown in the specimens from the Bishops Court Quarry in which the K_{max} axes are transverse to the aeolian foresets (Edwards & Scrivener 1999).

Mineralogical origin of magnetic properties

In summary, the magnetisation in these units is carried dominantly by haematite, with a likely large range of grain size from superparamagnetic (pigmentary) haematite to larger (specularite) particles of remanence carrying haematite. Magnetite may make a trace contribution. A strong control on the concentration of haematite is related to the clay and silt content, and perhaps also the concentration of volcanic rock detritus. The pigmentary haematite appears to have a multiphase origin, ranging from possible pre-deposition to late diagenetic, a typical feature of European Permian red beds (Turner *et al.* 1995; 1999). Largely detrital, specular haematite, varies in amounts relating to the degree of sediment sorting and the sediment supply. In the breccia units the maximum susceptibility axes reflect palaeocurrent-parallel trends, shown by clast imbrication directions. In aeolian transported sediments, the transverse trends in K_{max} axes reflect lee-face transport on dune slip faces. In the lacustrine mudstones the K_{max} directions may represent wave-produced (or perhaps wind-related?) grain orientations in the lake playa systems hence, the AMS shows a primary depositional fabric (unaffected by tectonism), probably carried mostly by haematite.

Palaeomagnetic Results

The majority of the 250 specimens demagnetised show little change in K_{lf} during demagnetisation, although the mudstones (particularly from the Littleham Mudstone Fm) tend to show alteration at >600^{o}C, with lower temperature alteration in some specimens (Fig. 6). In some

specimens, this alteration obscures the recovery of the remanence at higher demagnetisation temperatures.

Demagnetisation isolates two remanence components. Firstly, a positive, often northerly, steeply inclined component (Component A), between room temperature and often up to 350°C, but sometimes up to 500-600°C (Fig. 8). This component is more northerly in specimens from the Aylesbeare Mudstone Gp (Fisher mean, 005°, +59°, k= 7.7, Ns=135), but more southerly in specimens from the Exeter Gp (Fisher mean, 010°, +82°, k=6.7, Ns=44; see supplementary data). This component is more prevalent in the Aylesbeare Mudstone Gp (79% of specimens) compared to the Exeter Gp (56% of specimens), in which it is most prevalent in specimens from the Dawlish Sandstone Fm. It does not correspond in direction particularly well to the expected modern dipole field (i.e. inclination of 68°) and probably represents a composite component comprising mostly a Brunhes (viscous?) magnetisation plus the characteristic remanence. In 10% of samples from the Aylesbeare Mudstone Gp, this was the only component present. In the Exeter Gp 15% of specimens are dominated by this component, the bulk of these being from the Dawlish Sandstone Fm.

A second component is recognised between about 400 and 650-700 °C that is a northerly, positively inclined or southerly, negatively inclined direction (Fig. 8), interpreted as the characteristic remanence (ChRM). In the Littleham Mudstone Fm the unblocking temperature range of this component is mostly above 500°C- 600°C, whereas in specimens from the Exeter Gp, the unblocking of the ChRM often starts at temperatures of ~400°C. Some 52% of specimens (49% in Aylesbeare Mudstone Gp and 57% in Exeter Gp) had suitable linear trajectory ChRM line fits (here termed 'S-type' data; Fig. 8). This S-type demagnetisation behaviour was visually classified into three quality classes, S1, S2 and S3 (Figs. 8, 9). The mean α_{95} linear fits and ρ for these classes indicate the generally larger model variance required to accommodate the less quality line-fits (see supplementary data). Average confidence cone angles for these line-fit classes vary from 3.2 to 13.9°. The mean directions for the ChRM line-fits pass the reversal test (McFadden & McElhinney 1990), for all except those from the Littleham Mudstone Fm (Table 1; Fig. 9a).

Some 28% of specimens displayed great circle trends, of varying arc length, towards interpreted Permian reverse and normal polarity directions (here referred to as T-type demagnetization

behaviour; Fig. 8). This T-type behaviour was visually classified into three quality classes, T1, T2 and T3, based on the visual length and scatter of the demagnetisation points about the great circle, with T1 being the best quality. The mean α_{95} for the poles to the fitted planes, for these three data classes range from 9 to 20° (see supplementary data). These great circle fits included the origin in 67% of these cases.

Data from the Dawlish Sandstone Fm yield the least well-defined results, particularly those from Bishops Court Quarry, which are dominated by component A. These samples also display mainly low blocking temperatures (i.e. the NRM is largely demagnetised by ~500°C). Some specimens from this locality could be AF demagnetised, indicating that either these sandstones originally had no haematite, or more likely a substantial proportion of haematite had been removed, possibly by Quaternary ground water flow (e.g. Johnson *et al*. 1997). Notably, those samples that did not retain a ChRM generally lacked specular haematite particles in thin section, whereas samples of aeolian sandstone which possessed a ChRM often possessed specularite in small amounts. Hence, the poor palaeomagnetic behaviour in the Bishops Court Quarry samples is due to a paucity of specularite, and the dominance of pigment-dominated magnetisations, like Permian aeolian sandstones such as the Penrith Sandstone (Turner *et al.* 1995).

Mean directions and paleopoles

As well as the conventional means using the ChRM directions (Fig. 9), mean directions were also determined using 'specimen-based' means, by combining the great circle paths with the specimen line-fit ChRM (Table 1), to produce combined means using the method of McFadden & McElhinney (1988). This method determines a mean direction, by including the 'fixed-point' ChRM directions, and those points on the projected great circles, which maximise the resultant length (i.e. points on the great circle which are closest to the combined mean direction). These means are broadly similar to the line-fit ChRM means, except that for the Dawlish Sandstone and Exe Breccia, which have steeper inclination and greater dispersion (Table 1). The great-circle combined means pass the reversal test for the Littleham Mudstone Fm, Exmouth Mudstone and Sandstone Fm, and Dawlish Sandstone plus Exe Breccia formations (Table 1). Using the line-fit ChRM directions alone, the combined mean directions for the Aylesbeare Mudstone and Exeter groups pass the reversal test (Table 1).

453 The S-class ChRM directions for the Exeter Gp, pass the fold test, indicating the pre-folding
454 nature of the magnetisations (Fig. 9b). The fold test of McFadden (1990) produced an f-statistic
455 (F [6,82]) of 1.90. Likewise, these data pass the DC fold test of Enkin (2003), with best
456 unfolding at 93.5%, with a 95% confidence interval of ±25.2%. A progressive unfolding test
457 (Watson & Enkin 1993) indicated best unfolding at 78%, with 95% confidence intervals on the
458 percent unfolding of 34% to 114% (Fig. 9b).
459
460 The virtual geomagnetic pole (VGP) data is consistent with other Permian data from stable-
461 Europe, confirming the Permian age of these magnetisations. The mean direction for the Exeter
462 Gp produces a virtual geomagnetic pole (VGP) similar to stable-Europe sediments from the
463 youngest part of the KRPS (see Supplementary Data), although the mean is slightly to the east of
464 the European apparent polar wander path of Torsvik & Cocks (2005). The Exeter Volcanic
465 Rocks VGP of Zijderveld (1967) is similar to that from the Aylesbeare Mudstone Gp (Table 1),
466 whereas the VGP pole for the Exeter Gp sediments from this study, is displaced slightly more to
467 the east (see Supplementary Data).

468 ## Magnetostratigraphic Interpretation

469 The line-fit ChRM directions from the Aylesbeare Mudstone Gp (and Exe Breccia Fm) were
470 converted to virtual geomagnetic pole (VGP) latitude using the line-fit ChRM mean in Table 1
471 (Figs. 10a,b (iii)). For those specimens that had no line-fit, the point on their great circle nearest
472 this mean, were used for calculating the VGP latitude (Fig. 10). All specimens were also
473 assigned a polarity quality (Fig. 10a,b (ii)) based on the quality of demagnetisation behaviour
474 and, if from T-class specimens, the length and end point position of the great circle trend (similar
475 to the procedures used by Ogg & Steiner 1991; Hounslow & McIntosh 2003). One specimen of
476 good-quality polarity (i.e. S-Type) was sufficient to define the horizon polarity, whereas with
477 specimens of poorer quality at least two are required (Figs. 4, 10). Some 12% of specimens failed
478 to yield data which could be used to determine horizon polarity (10% in Aylesbeare Mudstone
479 Gp, 15% in Exeter Gp) and eight horizons failed to yield any specimens which could reliably be
480 used to determine magnetic polarity (Figs. 4, 5). Most of these are from sandstones, with most of
481 these in the Dawlish Sandstone Fm at Bishops Court Quarry (Fig. 4).
482
483 All the samples collected from below the Exe Breccia Fm are of reverse polarity, with those
484 sections situated stratigraphically above the Langstone Rock outcrop having both reverse and

485 normal polarity (Figs. 4, 5). The single sample from the Knowle Sandstone Fm (Fig. 2; Table 1)
486 likewise confirms the reverse polarity results from the age-equivalent Exeter Volcanic Rocks
487 found by Creer (1957), Zijderveld (1967) and Cornwall (1967). Significantly, two sites in the
488 Torbay Breccia Fm sampled in the reconnaissance study of Cornwall (1967) produced reverse
489 polarity, suggesting that reverse polarity probably dominates to the base of the Exeter Gp.
490
491 Major magnetozone reverse and normal couplets have been numbered (Fig. 10) from the base of
492 the first normal polarity samples in the Exe Breccia Fm, using the prefix EA (for Exeter-
493 Aylesbeare). The magnetic polarities of six magnetozones are defined with multiple specimens
494 from a single sampling horizon (EA3n.1r, EA3n.2r, EA5n.1r), and EA3r.1n is defined with a
495 single specimen of S-class behaviour (Fig. 10b).

496 ## Discussion

497 The major geomagnetic polarity marker in the Permian is the end of the Kiaman reverse polarity
498 Superchron, which has been comprehensively studied since the 1950's in Russian successions
499 (Molostovsky 1983; Burov *et al*. 1998). Studies on marine fossil-bearing rocks which
500 demonstrate the end of the Kiaman superchron are discontinuous studies in the SW USA (Steiner
501 2006), and Japan (Kirschvink *et al.* 2015), along with studies on successions in China (Steiner *et*
502 *al*. 1989; Embleton *et al*. 1996). The overlying reverse and normal polarity Illawarra Superchron,
503 has been investigated in marine successions in the Salt Range in Pakistan, China and Iran (Haag
504 & Heller 1991; Gallet *et al*. 2000; Jin *et al*. 2000; Steiner 2006), along with flood-basalts in
505 China (Ali *et al*. 2002; Zheng *et al.* 2010). Studies on non-marine rocks from the Illawarra
506 Superchron have been extensive in Russia, on outcrop and borehole material (Molostovsky 1983;
507 Burov *et al*. 1998) and core material from the Southern Permian Basin (Menning et al. 1988;
508 Nawrocki 1997; Turner *et al*. 1999; Lawton & Roberson 2003; Szurlies 2013). These studies
509 together allow the magnetic polarity stratigraphy (Fig. 11) to be defined through the Roadian to
510 Changhsingian (Steiner 2006; Hounslow submitted). The base of the Illawarra superchron is in
511 the lower to mid Wordian, based on magnetostratigraphic data from the Grayburg Fm in Texas
512 and New-Mexico (Steiner 2006) and limestones from Japan (Kirschvink *et al.* 2015).
513
514 Magnetostratigraphic studies in the southern Permian Basin well Mirow 1/1a/74 (Menning et al.
515 1988; Langereis *et al*. 2010), and wells in Poland (Nawrocki 1997) show a long-duration reverse
516 polarity interval (equivalent to MP3r –UP1r interval), with under and overlying mixed polarity-

517 intervals (Fig. 11). The normal magnetozones in the Lower Drawa Fm and Havel Subgroup are
518 probably equivalent with the MP1n to MP3n interval in the GPTS of Hounslow (submitted).
519 Equivalent normal magnetozones in the Notec and Hannover formations, are more fully
520 expressed by studies of the Lower Leman Sandstone, from the Johnston and Jupiter field in the
521 southern North Sea (Turner *et al*. 1999; Lawton & Roberson 2003; Fig. 11). These correlations
522 are constrained by the overlying Zechstein, and indicate that the Zechstein successions are
523 entirely Changhsingian in age, rather than as old as early Wuchiapingian, as suggested by the
524 conodonts *Merrillina divergens* and *Mesogondolella britannica* (Korte *et al.* 2005; Legler *et al*.
525 2005; Słowakiewicz *et al*. 2009), and the synthesis of Szurlies (2013). Like the
526 magnetostratigraphic interpretation here (Fig. 11), Sr-isotope data indicates a short duration for
527 the Zechstein of ~ 2 Ma, with a likely age range of 255-251.5 Ma, placing it firmly in the
528 Changhsingian (Denison & Peryt 2009). Attempts at dating the Kupferschiefer at the base of the
529 Zechstein (Z1 cycle) have failed to yield consistent results, with Re-Os ages giving wide 95%
530 confidence intervals (Pašava *et al.* 2010).
531
532 Four pieces of information have allowed the Exeter Gp succession to be assigned to the Permian.
533 1) Volcanic units interbedded with the Knowle Sandstone of the Exeter area, and similar units
534 equivalent to the Thorverton Sandstone and Bow Breccia in the Crediton Trough, have Ar-Ar
535 ages of 291- 282 Ma (Edwards & Scrivener 1999). Volcanic clasts in the breccia units give
536 Ar-Ar dates of 280 Ma. This suggests the volcanism and associated interbedded sediments
537 are late Sakmarian through to late Artinskian in age, using the timescale of Henderson *et al.*
538 (2012).
539 2) The Dartmoor Granite has Rb-Sr, U-Pb and Ar-Ar ages of 280 ±1 Ma (Scrivener 2006),
540 placing its formation in the latest Artinskian (timescale of Henderson *et al*. 2012). Clasts of
541 the granite begin to occur in the unroofing succession of the Teignmouth and Heavitree
542 Breccias (Dangerfield & Hawkes 1969; Edwards *et al*. 1997), indicating that these breccias
543 were deposited several millions years after the granite formation, in order to allow time for
544 granite unroofing.
545 3) Miospore assemblages containing *Lueckisporites virkkiae*, occur from the Whipton Fm,
546 around Exeter, but also in younger units in the Crediton Trough, equivalent to the Alphington
547 and Heavitree Breccias (Edwards *et al*. 1997). Assemblages containing this miospore are
548 widespread in European Zechstein deposits and similar 'Thuringian' and Russian Tatarian-
549 age assemblages (Visscher 1973; Utting 1996). In the northern hemisphere, *Lueckisporites*

virkkiae has its first appearance in the latest Kungurian (Shu 1999; Mangerud 1994) to early Roadian (lower Kazanian in Russia; Utting 1996), but occurrences range into the latest Changhsingian.

4) The foot-print trace-fossil *Cheilichnus bucklandi*, found in the Dawlish Sandstone near Exeter (Edwards *et al*. 1997) suggests equivalence to the Germanic 'Rotliegend' (McKeever & Haubold 1996). However, this genus is restricted to aeolian dune units and is probably only vaguely indicative of the Permian (Lucas & Hunt 2006).

Constraints on the youngest possible age of the Aylesbeare Mudstone Gp are magnetostratigraphy and vertebrate fossils from the overlying Otter Sandstone Formation (Hounslow & McIntosh 2003; Benton 1997), which indicate the Sherwood Sandstone Gp is as old as early Anisian (Middle Triassic), and probably ranges down into the Olenekian of the Lower Triassic (Hounslow & McIntosh 2003; Hounslow & Muttoni 2010). Based on regional climate comparisons between the Budleigh Salterton Pebble Beds and the 'Conglomérate principal' of the Vosges region in NE France, Durand (2006) suggested a probable early Olenekian age for the Budleigh Salterton Pebble Beds Fm, generally consistent with the magnetostratigraphy.

This work detects the oldest normal magnetozone in the mid-parts of the Exe Breccia (i.e. EA1n), with a substantial thickness (perhaps up to ~1 to 1.5 km) of reverse polarity in the underlying parts of the Exeter Gp. Although we cannot locate the base of EA1n precisely due to lack of suitable outcrop, this normal magnetozone is the earliest evidence of the Illawarra Superchron (Fig. 11). EA1n is probably equivalent to early MP2n, or the normal polarity part of MP1. However, ~55 m of unsampled strata occur in the interval between our outcrops at the Exe Breccia- Dawlish Sandstone boundary (Figs. 4, 11). Therefore, it is possible the equivalent of the MP1n chron is within this unsampled interval. The end of the KRPS provides an important dating-point (267.1±0.8 Ma; Hounslow submitted) to the early-mid Wordian in the Middle Permian (Guadalupian). The oldest occurrence of the *Lueckisporites virkkiae* assemblage is found in the Whipton Fm, which suggests that this formation could be as old as latest Kungurian to early Roadian (~272 Ma; Henderson *et al.* 2012). This would give a minimum of ~8 Ma of exhumation time, between formation of the Dartmoor Granite, and the first granite detritus appearing in the Teignmouth- Heavitree breccias.

583 The overlying normal polarity magnetozone EA3n, is therefore likely to be equivalent to the
584 MP3n normal magnetozone in the upper and mid parts of the Capitanian (Fig. 11). The EA3r
585 magnetozone is equivalent to the MP3r to UP1r interval (in the lower part of the Wuchiapingian),
586 with the overlying normal magnetozones (i.e. EA4n to EA5n) equivalent to those in the upper
587 parts of the Wuchiapingian to basal Changhsingian (Fig. 11). Reverse magnetozone EA2r, in the
588 top of the Exe Breccia is probably the equivalent of MP2r in the basal Capitanian. Sub
589 magnetozone EA3r.1n in the Littleham Mudstone Fm is probably equivalent to UP1n in the
590 Wuchiapingian.

591 *Alternative Lower Triassic age models?*

592 The alternative Lower Triassic age of the Aylesbeare Mudstone Gp suggested by Warrington &
593 Scrivener (1990) and Edwards *et al*. (1997), is untenable using the magnetostratigraphy. To
594 evaluate their hypothesis using this data suggests the most likely early Triassic correlation model
595 would indicate EA3n is the age equivalent of the first Triassic magnetozone, LT1n (Fig. 11).
596 Therefore, the overlying EA3r to EA5n interval would extend into the earliest Olenekian, an
597 interval of some 1.4 Ma (Hounslow & Muttoni 2010). However, this seems unlikely for the
598 following reasons:
599
600 1) The local clast lithologies (e.g. murchisonite) seen in the breccia at the base of the Littleham
601 Mudstone Fm, are similar to those in the Exeter Gp, and very different to those found in the
602 Budleigh Salterton Pebble Beds (and other Lower Triassic units further north in the UK),
603 which contain Armorican-derived clasts and zircons from Cadomian basement (Cocks 1993;
604 Morton *et al.* 2013).
605 2) It would require a minimum hiatus of ~ 13-15 Ma between the Exe Breccia and the
606 Aylesbeare Mudstone Gp, which seems unlikely considering the apparently conformable
607 nature of the boundary between these formations in the Exe Estuary area.
608 3) If the hypothesis of Warrington & Scrivener (1990) was correct, it would predict numerous
609 normal polarity intervals (from the Illawarra superchron) below the Aylesbeare Mudstone Gp
610 but we have only found these in the Exe Breccia Fm with no evidence of normal polarity in
611 the underlying *c*.1 km of the Exeter Gp.
612 4) This Lower Triassic model would suggest a ~1.4 Ma duration for the EA3n to EA5n interval
613 requiring very large accumulation rates, comparable to the deepest grabens in the Southern

Permian Basin, north of the Variscan front, which there contain substantial thicknesses of Zechstein.

Wider regional implications

A consequence of these data is that it is now possible to assess the relationship of the SW England successions to the much better studied Rotleigend-II group in the Southern Permian Basin (Fig. 11). The magnetostratigraphy suggests a similarity in age of the Altmark unconformities with the Devon Permian sequence boundaries. The magnetic polarity stratigraphy from the Mirow, Czaplinek and Piła wells suggests that the Altmark III unconformity is roughly equivalent to the base of the Littleham Mudstone Fm (base of Pm5 sequence; Fig. 2), Altmark II, with the base of sequence Pm4 (Figs. 2, 11). Less certain is the correlation of the base of unit B in the Littleham Mudstone Fm, with Altmark IV. The base of sequence Pm3 probably relates to the Altmark I unconformity, which separates the Muritz Subgroup from the Havel Subgroup, across the Saalian unconformity, since underlying successions both contain volcanic units.

The calcrete and rhizoconcretion bearing sandstone, in the uppermost part of the Straight Point Sandstone Mbr, is unusual in that no other well developed palaeosols are seen in the remainder of these Permian successions. It is not until the mid Triassic (Anisian) Otter Sandstone Fm, that calcretes began to be widely developed in SW England. The Capitanian-Wuchiapingian boundary was an interval with dramatic, but poorly understood shifts in the global carbon cycle (Nishikane *et al.* 2014). A tentative reason for this palaeosol development is the rapid warming associated with increased CO_2 in the atmosphere (and associated increased evaporation rates to create calcretes; Alonso-Zarza 2003), that developed after the extinction at the Capitanian-Wuchiapingian boundary. The peak is associated with a negative $\delta^{13}C$ excursion (Chen *et al.* 2011; Nishikane *et al.* 2014) in the early Wuchiapingian, which corresponds closely to the early parts of MP3r (Zheng *et al.* 2010; Fig. 11).

The dramatic switch between breccia-dominated facies of the Exeter Gp to the mudstone-dominated facies of the Aylesbeare Mudstone Gp, occurs within the early Capitanian (Fig. 11). We tentatively relate this switch in facies to the Kamura cooling event (seen as a large positive $\delta^{13}C$ excursion during the Capitanian), which began in the early Capitanian (Isozaki *et al.* 2011). This has been associated with lows in atmospheric CO_2, and cooler oceanic surface waters in both the Panthalassa and Paleo-Tethys Oceans (Isozaki *et al.* 2011; Nishikane *et al.* 2014). This

cooling event may have allowed more moisture-bearing weather systems to penetrate further northwards into the heart of Pangaea, from the Paleo-Tethys, so allowing delivery of larger amounts of mud into the playa systems of the Aylesbeare Mudstone Gp.

The Southern Permian Basin, Parchim and Mirow formations shows a number of similarities to the Devon successions. The Parchim Fm dominantly comprises thick conglomeratic braidplain-type deposits, extending to sandflat and locally playa mudstone deposits in the basin centre (McCann 1998; Rieke *et al.* 2003). Tectonic control of facies was important during the Parchim Fm. Like the Exeter Group in sequence Pm3 (Fig. 2) the Parchim Fm has an earlier wetter phase and a later dryer phase (Rieke *et al.* 2003). This is overlain by the Mirow Fm which is characterized by the progradation of sand-prone fluvial facies with frequent claystones, over a much wider extent in the Southern Permian Basin than the Parchim Fm. The rarity of conglomerates (except at basin margins), with instead claystones (containing fossils indicative of freshwater conditions) and the dominance of sand-prone facies, is very different to the underlying Parchim Fm (McCann 1998). Hence, the start of the Mirow Fm sees a switch to climatically wetter conditions (Rieke *et al.* 2003), like those seen in the Aylesbeare Mudstone Gp. The coincidence in timing and the switch to wetter environmental conditions, seen in the Devon successions and German basins, suggests these major facies changes are climatically controlled.

Conclusions

The palaeomagnetic signal in the Exeter and Aylesbeare Mudstone groups is dominantly carried by haematite, whose mean directions pass the reversal test. The remanence in the Exeter Gp passes a fold test. The AMS indicates the fabric carried by haematite is detrital in origin. Reverse polarity dominates in the lower part of the Exeter Gp, with the start of the Illawarra superchron, in the Exe Breccia Fm dated to the early Wordian. Five normal-reverse couplets are found in the overlying sediments starting in the upper part of the Exe Breccia Fm (Langstone Mbr) and into the Aylesbeare Mudstone Gp. This magnetostratigraphic data allows the Exmouth Mudstone and Sandstone Fm to be assigned to the Capitainian to the earliest Wuchiapingian, and the overlying Littleham Mudstone Fm is earliest Wuchiapingian, to as young as the Wuchiapingian-Changhsingian boundary. With these data, the Permian successions in SW England are now the most precisely dated Permian succession in the UK, and if similar methods were used elsewhere, should provide the foundation for a much better understanding of other UK Permian basins. The

678 similarity in the timing between facies changes and sequence boundaries, here and those of the
679 Rotliegend-II Group in the Southern Permian Basin, indicates that palaeoclimatic change is a
680 fundamental metric in their subdivision. The question of the position of the Permo-Triassic
681 boundary in SW England has now been effectively resolved, and ironically corresponds to the
682 position taken by Victorian geologists such as Irving (1888).

683 Acknowledgements

684 This work was part-funded by a British Geological Survey- University collaboration grant.
685 Richard Scrivener led fieldwork to the Crediton Trough, and Paulette Posen assisted during
686 fieldwork to the Exeter Gp. Robert Hawkins and Laurence Thistlewood measured some of the
687 samples. Sylvie Bourquin and Antoine Bercovici assisted in the fieldwork in 2007. Simon Chew
688 drafted some of the figures. The MOD kindly allowed access to the Straight Point firing range. A
689 reviewer Tim Raub provided constructive suggestions for improvement.

690 References

691 Ali, J. R, Thompson, G. M., Song, X. & Wang, Y. 2002. Emeishan Basalts (SW China) and the
692 'end-Guadalupian' crisis: magnetobiostratigraphic constraints. *Journal of the Geological*
693 *Society*, **159**, 21-29.
694 Alonso-Zarza, A. M. 2003. Palaeoenvironmental significance of palustrine carbonates and
695 calcretes in the geological record. *Earth-Science Reviews*, **60**, 261-298.
696 Barton, C. M., Woods, M. A., Bristow, C. R., Newell, A. J., Westhead, R. K., Evans, D. J.,
697 Kirby, G. A., & Warrington, G. 2011. *The geology of south Dorset and south-east Devon*
698 *and its World Heritage Coast.* Special Memoir of the British Geological Survey, Sheets 328,
699 341/342, 342/343 and parts of 326/340, 327, 329 and 339. HMSO, London
700 Bateson, J. H. & Johnson, C. C. 1992. *Reduction and related phenomena in the New Red*
701 *Sandstone of south-west England*, British Geological Survey, Technical report WP/92/1.
702 Benton, M. J., Cook, E., & Turner, P. 2002. *Permian and Triassic red beds and the Penarth*
703 *Group of Great Britain*. Geological Conservation Review Series. Joint Nature
704 Conservation Committee, Peterborough.
705 Benton, M. J. 1997. The Triassic reptiles from Devon. *Proceedings of the Ussher Society*, **9**, 141-
706 152.
707 Burov, B. V., Zharkov, I. Y., Nurgaliev, D. K., Balabanov, Yu. P., Borisov, A. S. & Yasonov, P.
708 G. 1998. Magnetostratigraphic characteristics of Upper Permian sections in the Volga

709 and the Kama areas. *In:* Esaulova, N. K., Lozonsky, V. R., Rozanov, A. Yu. (eds).
710 *Stratotypes and reference sections of the Upper Permian in the regions of the Volga and*
711 *Kama Rivers*. GEOS, Moscow, 236-270.
712 Butler, M. 1998. The geological history and the southern Wessex Basin- a review of new
713 information from oil exploration. *In:* Underhill, J. R. (ed.), *Development, evolution and*
714 *petroleum geology of the Wessex Basin*. Geological Society London Special Publication
715 **133**, 67-86.
716 Carter, A. Yelland, A. Bristow, C. & Hurford, A. J. 1995. Thermal histories of Permian and
717 Triassic basins in Britain derived from fission track analysis. *In:* Boldy, S.A. R. (ed.),
718 *Permian and Triassic Rifting in Northwest Europe*, Geological Society Special
719 Publication, **91**, 41-56.
720 Chapman, T. J. 1989. The Permian to Cretaceous structural evolution of the Western Approaches
721 Basin (Melville sub-basin), UK. *In:* M.A. Cooper (ed.), *Inversion Tectonics,* Geological
722 Society, London, Special Publications; **44**, 177-200.
723 Chen, B., Joachimski, M. M., Sun, Y., Shen, S. & Lai, X. 2011. Carbon and conodont apatite
724 oxygen isotope records of Guadalupian–Lopingian boundary sections: Climatic or sea-
725 level signal? *Palaeogeography, Palaeoclimatology, Palaeoecology*, **311**, 145-153.
726 Cocks, L. R. M. 1993. Triassic pebbles, derived fossils and the Ordovician to Devonian
727 palaeogeography of Europe. *Journal Geological Society London*, **150**, 219-226.
728 Cornwall, J. D. 1967. Palaeomagnetism of the Exeter Lavas, Devonshire. *Geophys. Journal*
729 *Royal Astro. Soc*., **12**, 181-196.
730 Creer, K. M. 1957. The Natural Remanent Magnetization of Certain Stable Rocks from Great
731 Britain. *Philosophical Transactions of the Royal Society of London. Series A, Mathematical*
732 *and Physical Sciences*, **250**, 111-129.
733 Dangerfield, J. & Hawkes, J. R. 1969. Unroofing of the Dartmoor Granite and possible
734 consequences with regard to mineralization. *Proc. Ussher Soc.,* **2**, 122-131.
735 Denison, R. E. & Peryt, T. M. 2009. Strontium isotopes in the Zechstein (Upper Permian)
736 anhydrites of Poland: evidence of varied meteoric contributions to marine brines. *Geological*
737 *Quarterly*, **53**, 15
738 Durand, M. 2006. The problem of the transition from the Permian to the Triassic Series in
739 southeastern France: comparison with other Peritethyan regions. *In:* Lucas, S. G., Cassinis,
740 G. & Schneider J.W. (eds) *Non-Marine Permian Biostratigraphy and Biochronology*,
741 Geological Society, London, Special Publications, **265**, 281-296.

742 Durrance, E. M., Meads, R. E., Ballard, R. R. B. & Walsh, J. N. 1978. Oxidation state of iron in
743 the Littleham Mudstone Formation of the new red sandstone series (Permian-Triassic) of
744 southeast Devon, England. *Geological Society of America Bulletin*, **89**, 1231-1240.
745 Edwards, R. A. & Scrivener, R. C., 1999. *Geology of the country around Exeter. Memoir of the*
746 *British Geological Survey, Sheet 325 (England and Wales)*, HMSO, London.
747 Edwards, R. A., Warrington, G., Scrivener, R. C., Jones, N. S., Haslam, H. W. & Ault, L. 1997.
748 The Exeter Group, south Devon, England: a contribution to the early post-Variscan
749 stratigraphy of northwest Europe. *Geological Magazine*, **134**, 177-197.
750 Ellwood, B. B. & Howard, J. H. 1981. Magnetic fabric development in an experimentally
751 produced barchan dune. *Journal of Sedimentary Research*, **51**, 97-100.
752 Embleton, B. J. J., McElhinny, M. W., Zhang Z. & Li Z. X. 1996. Permo-Triassic
753 magnetostratigraphy in China: the type section near Taiyuan, Shanxi Province, North
754 China. *Geophys. J. Int.* **126**: 382–388
755 Enkin, R. J. 2003. The direction- correction tilt test: an all purpose tilt/fold test for
756 palaeomagnetic studies. *Earth Planet. Sci. Lett*., **212**, 151-166.
757 Evans, C. D. R. 1990. *The geology of the western English Channel and its western Approaches.*
758 *UK Offshore regional report*. British Geological Survey, HMSO, London.
759 Frank, U. and Nowaczyk, N. R. 2008. Mineral magnetic properties of artificial samples
760 systematically mixed from haematite and magnetite. *Geophys. J. Int.* **175**, 449–461.
761 Gallet, Y., Krystyn, L., Besse, J., Saidi, A. & Ricou, L-E. 2000. New constraints on the upper
762 Permian and Lower Triassic geomagnetic polarity timescale from the Abadeh section
763 (central Iran). *Journal of Geophysical Research*, **105**, 2805-2815.
764 Gallois, R.W. 2014. The position of the Permo-Triassic boundary in Devon, UK. *Geoscience in*
765 *South-West England*, **13**, 328-338.
766 Haag, M. & Heller, F. 1991. Late Permian to Early Triassic magnetostratigraphy. *Earth Planet.*
767 *Sci. Letter*, **107**, 42-54.
768 Hamblin, R. J. O., Crosby, A., Alson, R. S., Jones, S. M., Chadwick, R. A., Penn, I. E. & Arthur,
769 M. J. 1992. *United Kingdom off-shore report: the geology of the English Channel*.
770 British Geological Survey, HMSO, London.
771 Harvey, M. J. Stewart, S. A., Wilkinson, J.J., Ruffell, A. H. & Shall, R. K. 1994. Tectonic
772 evolution of the Plymouth Bay Basin. *Proceedings of the Ussher Society*, **8**, 271-278.

773 Henderson, C. M., Davydov, V. I. & Wardlaw, B. R. 2012. The Permian Period. *In:* Gradstein,
774 F.M., Ogg, J.G, Schmitz, M.D. & Ogg, G.M (eds), *The geologic time scale 2012*, vol. 2,
775 Elsevier, Amsterdam, 653-679.
776 Henson, M. R. 1972. The form of the Permo-Triassic basin in south-east Devon. *Proc. Ussher*
777 *Soc*. **3**, 447-457.
778 Hounslow, M.W. & McIntosh, G. 2003. Magnetostratigraphy of the Sherwood Sandstone Group
779 (Lower and Middle Triassic): South Devon, U.K.: Detailed correlation of the marine and
780 non-marine Anisian. *Palaeogeogr. Palaeoclimat. Palaeoecol.,* **193**, 325-348.
781 Hounslow M.W. & Muttoni G. 2010. The geomagnetic polarity timescale for the Triassic:
782 Linkage to stage boundary definitions. *In:* Lucas, S. G. (ed.) *The Triassic timescale*.
783 Special Publication of the Geological Society, **334**, 61-102.
784 Hounslow, M. W. (submitted). Palaeozoic geomagnetic reversal rates following superchrons
785 have a fast re-start mechanism. *Nature Communications*.
786 Irving, A. 1888. The red-rock series of the Devon Coast section. *Quart. J. geol. Soc.*, **44**, 149-
787 163.
788 Isozaki, Y., Aljinovic, D. & Kawahata, H. 2011. The Guadalupian (Permian) Kamura event in
789 European Tethys. *Palaeogeography, Palaeoclimatology, Palaeoecology* **308**, 12–21.
790 Jin, Y. Shang, Q. & Cao, C. 2000. Late Permian magnetostratigraphy and its global correlation.
791 *Chinese Science Bulletin*, **45**, 698-705.
792 Johnson, S. A., Glover B. W. & Turner, P. 1997. Multiphase reddening and weathering events in
793 Upper Carboniferous red beds from the English West Midlands. *Journal of the*
794 *Geological Society*, **154**, 735-745.
795 Kent, J. T., Briden, J. C. & Mardia, K. V. 1983. Linear and planar structure in ordered
796 mulivariate data as applied to progressive demagnetisation of palaeomagnetic remanence.
797 *Geophysical Journal Royal Astronomical Society*, **81**, 75-87.
798 Kirschvink, J. L., Isozaki, Y., Shibuya, H., Otofuji, Y. I., Raub, T. D., Hilburn, I. A., Kasuya, T.,
799 Yokoyama, M. & Bonifacie, M. 2015. Challenging the sensitivity limits of
800 Paleomagnetism: Magnetostratigraphy of weakly magnetized Guadalupian–Lopingian
801 (Permian) Limestone from Kyushu, Japan. *Palaeogeography, Palaeoclimatology,*
802 *Palaeoecology*, **418**, 75-89.
803 Korte, C., Kozur, H. W. & Veizer, J. 2005. δ^{13}C and δ^{18}O values of Triassic brachiopods and
804 carbonate rocks as proxies for coeval seawater and palaeotemperature. *Palaeogeography,*
805 *Palaeoclimatology, Palaeoecology*, **226**, 287-306.

806 Kostadinova M., Jordanova N., Jordanova D. & Kovacheva M. 2004. Preliminary study on the
807 effect of water glass impregnation on the rock-magnetic properties of baked clay. *Studia*
808 *Geophysica et Geodaetica*, **48**, 637-646.
809 Laming, D. J. C. 1966. Imbrications, palaeocurrents and other sedimentary features in the Lower
810 New Red Sandstone, Devonshire, England. *Journal of Sedimentary Petrology*, **36**, 940-
811 959.
812 Laming, D. J. C. 1969. A guide to the New Red Sandstone of Tor Bay, Petitor and Shaldon.
813 Report *Transaction of Devonshire Association of Science, Literature and Art*, **101**, 207-
814 218.
815 Laming, D. J. C. 1982. The New Red Sandstone. *In:* Durrance, E. M. & Laming, D. J. C. (eds)
816 *The geology of Devon*. University of Exeter Press, Exeter, 148-178,
817 Laming, D. J. C. & Roche, D. P. 2013. Faulting in Permo-Triassic strata and buried channels
818 revealed by excavation of the Lympstone-Powderham tunnel, Exe Estuary, Devon.
819 *Geoscience in South-West England*, **13**, 244.
820 Langereis, C. G., Krijgsman, W., Muttoni, G. & Menning, M. 2010. Magnetostratigraphy -
821 concepts, definitions, and applications. *Newsletters on Stratigraphy*, **43**, 3, 207-233
822 Lawton, D. E. & Roberson, P. P. 2003. The Johnston Gas Field, Blocks 43/26a, 43/27a, UK
823 Southern North Sea. *In:* Gluyas, J. & Hichens, H. M. (eds), *United Kingdom Oil and Gas*
824 *Fields, Commemorative Millennium Volume*. Geological Society London Memoir, **20**,
825 749-759.
826 Legler, B., Gebhardt, U. & Schneider, J. W. 2005. Late Permian non marine to marine
827 transitional profiles in central southern Permian Basin, northern Germany. *Int. Journal of*
828 *Earth Sciences*, **94**, 851-862.
829 Leveridge, B. E. Scrivener, R. C. Goode, A. J. J. & Merriman, R. J. 2003. *Geology of the*
830 *Torquay district, a brief explanation of the geological map sheet 350 Torquay*.
831 Keyworth: British Geological Survey, HMSO, London.
832 Løvlie, R. & Torsvik, T. 1984: Magnetic remanence and fabric properties of laboratory-deposited
833 hematite-bearing red sandstone. *Geophysical Research Letters*, **11**, 229-232.
834 Lowrie, W. 1990. Identification of ferromagnetic minerals in a rock by coercivity and unblocking
835 temperature properties. *Geophysical Research Letters*, **17**, 159-162.
836 Lucas, S. G. & Hunt, A. P. 2006. Permian tetrapod foorptints: biostratigraphy and biochronology.
837 *In:* Lucas, S.G. Cassinis, G. & Schneider, J.W. (eds), *Non-marine Permian*

biostratigraphy and biochronology, Geological Society, London Special Publications, **265**, 179-200.

Mangerud, G. 1994. Palynostratigraphy of the Permian and lowermost Triassic succession, Finnmark Platform, Barents sea. *Review of Palaeobotany & Palynology*, **82**, 317-349.

McCann, T., Pascal, C., Timmerman, M. J., Krzywiec, P., López-Gómez, J., Wetzel, L. & Lamarche, J. 2006. Post-Variscan (end Carboniferous-Early Permian) basin evolution in western and central Europe. *In:* Gee, D. G. & Stephenson, R. A. (eds) *European Lithosphere Dynamics*. Geological Society London Memoirs, **32**, 355–388.

McCann, T. 1998. Sandstone composition and provenance of the Rotliegend of the NE German Basin. *Sedimentary Geology*, **116**, 177-198.

McFadden, P. L. 1990. A new fold test for palaeomagnetic studies. *Geophysical Journal International*, **103**, 163-169.

McFadden, P. L. & McElhinney, M. W. 1988. The combined analysis of remagnetisation circles and direct observations in palaeomagnetism. *Earth Planetary Science Letters*, **87**, 161-172.

McFadden, P. L. & McElhinny, M. W. 1990. Classification of the reversal test in palaeomagnetism. *Geophysical Journal International*, **103**, 725-729.

McKeever, P. M. & Haubold, H. 1996. Reclassification of vertebrate trackways from the Permian of Scotland and related forms from Arizona and Germany. *Journal of Paleontology*, **70**, 1011-1022.

McKie, T. & Williams, B. P. J. 2009. Triassic palaeogeography and fluvial dispersal across the northwest European Basins. *Geological Journal*, **44**, 711-741.

Menning, M., Katzung, G. & Lützner, H. 1988. Magnetostratigraphic investigations in the Rotliegendes (300-252 Ma) of Central Europe. *Z. geol. Wiss., Berlin*, **16**, 1045-1063.

Merefield, J. R., Brice, C. J. & Palmer, A. J. 1981. Caesium from former Dartmoor volcanism: its incorporation in NewRed sediments of SW England. *Journal of the Geological Society*, **138,** 145-152.

Molostovsky, E. A. 1983. *Paleomagnetic stratigraphy of the eastern European part of the USSR*. University of Saratov, Saratov [In Russian].

Morton, A. C., Hounslow, M. W. & Frei, D. 2013. Heavy-mineral, mineral-chemical and zircon-age constraints on the provenance of Triassic sandstones from the Devon coast, southern Britain. *Geologos* **19**, 67–85.

870 Nawrocki, J. 1997. Permian to early Triassic magnetostratigraphy from the central european
871 basin in poland: Implications on regional and worldwide correlations. *Earth. Planet. Sci*
872 *Lett.,* **152**, 37-58.
873 Newell, A. J. 2001. Bounding surfaces in a mixed aeolian-Fluvial system (Rotliegend, Wessex
874 Basin, SW UK). *Marine & Petroleum Geology*, **18**, 339-347.
875 Nishikane, Y., Kaiho, K., Henderson, C. M., Takahashi, S. & Suzuki, N. 2014. Guadalupian–
876 Lopingian conodont and carbon isotope stratigraphies of a deep chert sequence in Japan.
877 *Palaeogeography, Palaeoclimatology, Palaeoecology*, **403**, 16-29.
878 Ogg, J. G. & Steiner, M. B. 1991. Early Triassic polarity time-scale: integration of
879 magnetostratigraphy, ammonite zonation and sequence stratigraphy from stratotype
880 sections (Canadian Arctic Archipelago). *Earth and Planetary Science Letters*, **107**, 69–
881 89.
882 Ormerod- Wareing, G. 1875. On the Murchisonite beds of the Estuary of the Exe and an attempt
883 to classify the beds of the Trias thereby. *Quart, J. Geol. Soc. Lond.*, **31**, 346-354.
884 Park, M. E., Cho, H., Son, M. & Sohn, Y. K. 2013. Depositional processes, paleoflow patterns,
885 and evolution of a Miocene gravelly fan-delta system in SE Korea constrained by
886 anisotropy of magnetic susceptibility analysis of interbedded mudrocks. *Marine and*
887 *Petroleum Geology*, **48**, 206-223.
888 Pašava, J., Oszczepalski, S. & Du, A. 2010. Re–Os age of non-mineralized black shale from the
889 Kupferschiefer, Poland, and implications for metal enrichment. *Mineralium Deposita*,
890 **45**, 189-199.
891 Rieke, H., McCann, T., Krawczyk, C. M. & Negendank, J. F.W. 2003. Evaluation of controlling
892 factors on facies distribution and evolution in an arid continental environment: an
893 example from the Rotliegend of the NE German Basin. *In:* McCann, T. & Saintot. A.
894 (eds) *Tracing Tectonic Deformation Using the Sedimentary Record.* Geological Society,
895 London, Special Publications, **208**, 71- 94.
896 Roscher, M. & Schneider, J. W. 2006. Permo-Carboniferous climate: Early Pennsylvanian to late
897 Permian climate development of central Europe in a regional and global context. *In:*
898 Lucas, S. G. Cassinis, G. & Schneider, J. W. (eds) *Non-marine Permian biostratigraphy*
899 *and biochronology*, Geological Society, London Special Publication, **265**, 15-38.
900 Schwarzacher, W. 1951. Grain orientation in sands and sandstones. *Journal of Sedimentary*
901 *Research*, 21, 162-172.

902 Scrivener, R. C. 2006. Cornubian granites and mineralization in SW England. *In:* Brenchley, P. J.
903 & Rawson, P. F. *Geology of England and Wales*. Geological Society of London
904 Publication, Bath, 257-267.
905 Selwood, E. B. Edwards, R. A., Simpson, S., Chesher, J. A. & Hamblin, R. A. 1984. *Geology of*
906 *the country around Newton Abbot. Memoir for 1:50,000 geological sheet 339*, British
907 Geological Survey, HMSO, London.
908 Shen, S-Z., Henderson, C. H., Bowring, S. A., Cao1, C-Q. Wang, Y., Wang, W., Zhang, H.,
909 Zhang, Y-C. & Mu, L. 2010. High-resolution Lopingian (Late Permian) timescale of
910 South China. *Geological Journal*, **45**, 122–134.
911 Shu, O. 1999. A brief discussion on the occurrences of *Scutasporites unicus* and *Lueckisporites*
912 *virkkiae* complexes in the northern hemisphere. *Permophiles*, **33**, 21-23.
913 Słowakiewicz, M., Kiersnowski, H. & Wagner, R. 2009. Correlation of the Middle and Upper
914 Permian marine and terrestrial sedimentary sequences in Polish, German and USA
915 Western Interior Basins with reference to global time markers. *Palaeoworld*, **18**, 193-
916 211.
917 Steiner, M. 2006. The magnetic polarity timescale across the Permian-Triassic boundary. *In:*
918 Lucas, S. G. Cassinis, G. and Schneider, J. W. (eds)*, Non-marine Permian biostratigraphy*
919 *and biochronology*, Geological Society, London Special Publication, **265**, 15-38.
920 Steiner, M. B., Ogg, J., Zhang, Z. & Sun, S. 1989. The Late Permian/early Triassic magnetic
921 polarity time scale and plate motions of south China. *Journal Geophysical Research*, **94**,
922 7343-7363.
923 Strachan, R. A., Linnemann, U., Jeffries, T., Drost, K. & Ulrich, J. 2014. Armorican provenance
924 for the mélange deposits below the Lizard ophiolite (Cornwall, UK): evidence for Devonian
925 obduction of Cadomian and Lower Palaeozoic crust onto the southern margin of Avalonia.
926 *International Journal of Earth Sciences*, **103**, 1359-1383.
927 Szurlies, M., Bachmann, G. H., Menning, M., Nowaczyk, N. R. & Käding, K-C. 2003.
928 Magnetostratigraphy and high resolution lithostratigraphy of the Permian- Triassic boundary
929 interval in Central Germany. *Earth and Planetary Science Letters*, **212**, 263-278.
930 Szurlies, M. 2013. Late Permian (Zechstein) magnetostratigraphy in western and central Europe.
931 *In:* Gasiewicz, A. & Słowakiewicz, M. (eds), *Palaeozoic climate cycles: their evolutionary*
932 *and sedimentological impact.* Geological Society, London, Special Publications, **376**, 73-85.
933 Tarling, D. H. & Hrouda, F. 1993. *The magnetic anisotropy of rocks*. Chapman and Hall,
934 London.

935 Thomas, H. H. 1909. A contribution to the petrography of the New Red Sandstone in the West
936 of England. *Quarterly Journal of the Geological Society, London*, **65**, 229-245.
937 Timmerman, M. J. 2004. Timing, geodynamic setting and character of Permo-Carboniferous
938 magmatism in the foreland of the Variscan Orogen, NW Europe. *In:* Wilson, M.,
939 Neumann, E. -R., Davies, G. R., Timmerman, M. J., Heeremans, M. & Larsen, B. T.
940 (eds) *Permo-Carboniferous Rifting and Magmatism in Europe*, Special Publication
941 Geological Society, London, **223**, 41-74.
942 Torsvik T. H. & Cocks L. R. M. 2005. Norway in space and time: A Centennial cavalcade.
943 *Norwegian Journal of Geology*, **85**, 73-86.
944 Turner, P. 1979. The palaeomagnetic evolution of continental red beds. *Geological Magazine,*
945 **116**, 289-301.
946 Turner, P., Burley, S. D. Rey, D. & Prosser, J. 1995. Burial history of the Penrith Sandstone
947 (Lower Permian) deduced from the combined study of fluid inclusion and palaeomagnetic
948 data. *In:* Turner, P. & Turner, A. (eds) *Paleomagnetic applications in hydrocarbon*
949 *exploration*. Geological Society London Special Publications, **98**, 43-78.
950 Turner, P., Chandler, P., Ellis, D., Leveille, G. P. & Heywood, M. L. 1999. Remanance
951 acquisition and magnetostratigraphy of the Leman Sandstone Formation: Jupiter Fields,
952 southern North Sea. *In:* Tarling, D. H. & Turner, P. (eds) *Palaeomagnetism and diagenesis*
953 *in sediments*, Geological Society of London special publications, **151**, 109-124.
954 Ussher, W. A. E 1876. On the Triassic rocks of Somerset and Devon. *Quart Jour. Geol. Soc.*,
955 32, 367-394.
956 Ussher, W. A. E 1913. *The geology of the country around Newton Abbott: explanation of sheet*
957 *339.* Geological Survey of Great Britain. HMSO, London.
958 Visscher, H. 1973. The Upper Permian of western Europe—a palynological approach to
959 chronostratigraphy. *In:* Logan A. & Hills L.V. (eds) *The Permian and Triassic systems and*
960 *their mutual boundary*. Can. Soc. Pet. Geol. Mem., **2,** 200-219.
961 Warrington, G. & Scrivener, R. C. 1990. The Permian of Devon, England. *Review Palaeobotany*
962 *Palynology*, **66**, 263-272.
963 Watson, G. S & Enkin, R. J. 1993. The fold test in palaeomagnetism as a parameter estimation
964 problem. *Geophysical Research Letters*, **20**, 2135-3137.
965 Wills, L. J. 1970. The Triassic succession in the central Midlands in its regional setting. *Jour.*
966 *Geol. Soc. Lond.*, **126**, 225-283.

967 Zheng, L., Yang, Z., Tong, Y., & Yuan, W. 2010. Magnetostratigraphic constraints on two-stage
968 eruptions of the Emeishan continental flood basalts. *Geochemistry, Geophysics,*
969 *Geosystems*, **11**, doi:10.1029/2010GC003267.
970 Zijderveld, J. D. A. 1967. The natural remanent magnetisation of the Exeter Volcanic Traps
971 (Permian, Europe). *Tectonophysics*, **4**, 121-153.
972 Underhill, J. R. & Stoneley, R. 1998. Introduction to the development, evolution and petroleum
973 geology of the Wessex Basin. *In:* Underhill, J. R. (ed.) Development, Evolution and
974 Petroleum Geology of the Wessex Basin, Geological Society, London, Special
975 Publications, **133**, 1-18.
976 Utting, J., 1996. Palynology of the Ufimian and Kazanian Stages of Russian stratotypes, and their
977 comparison to the Word and Road of Canadian Arctic. *In:* Esaulova, N. K. & Lozovsky,
978 V. R. (eds) *Stratotypes and reference sections of the Upper Permian of regions of the*
979 *Volga and Kama Rivers*. Izd. “Ecocentr”, Kazan, 486-506.
980

Figure Captions

Fig. 1. Sketch map of the Permian-Triassic in SE Devon. Inset a) shows the study location within the UK, where grey=Lower Palaeozoic basement highs, dotted=Permian basins. CAB=Channel Approaches Basin, LRS=Lizard-Rhenish Suture, RHZ=Rheno-Hercynian Zone, STZ= Saxo-Thuringian Zone . In main map, numbers correspond to the sampling locations indicated in the Supplementary Data. Adapted from Selwood *et al*. (1984), Edwards *et al*. (1997). Sampling locations on coast indicated by } and in-land as ■.

Fig. 2. The stratigraphy of the Permian- Triassic around Exeter and the SE Devon coasts. Based on this work and Laming (1982), Selwood *et al*. (1984), Edwards & Scrivener (1999), Leveridge *et al*. (2003). Thicknesses of the coastal units is based on Selwood *et al*. (1984), Laming (1982) and this work. The chronology is based on Edwards *et al*. (1997), Edwards & Scrivenor (1999) and this work. The Torbay Breccia Formation occurs west of the Stickepath fault zone (SFZ, dashed in grey), and is divisible into an upper unit (the Paignton breccias, PB) probably equivalent to the Oddicombe Breccia Fm , and a lower unit composed of several separate breccias units. PTM=Petit Tor Member. Arrows indicate overstepping units.

Fig. 3. A) The erosional boundary between the Littleham Mudstone Fm (below) and the Budleigh Salterton Pebble Beds Fm (photo courtesy of Richard Porter), B) Immature calcrete and calcretised rootlets, top part of Straight Point Sandstone Member. C) Erosional boundary of breccia (base of arrow) at base of the Littleham Mudstone Fm, Littleham Cove (photo courtesy of Ian West). Scale arrow height=1.5 m. D) Unconformable boundary (marked in white) between the Watcombe Fm and the Oddicombe Breccia Fm, Whitsands Bay, hammer for scale. E) Detrital opaques (black) and pigmentary haematite grain coating (in red), fluvial sandstone, Dawlish Sandstone Fm, Dawlish Station section. The right hand side opaque (a haematised rock fragment) shows compactional deformation from surrounding framework grains. F) Detrital opaque showing indentation due to compaction into the surrounding quartz grains. Pigmentary haematite rims not present at opaque-quartz boundary. Fluvial sandstone in Dawlish Sandstone Fm. Pore spaces in blue. E) and F) scale bar is 100 μm.

Fig. 4. Section logs and summary palaeomagnetic data (horizon polarity, demagnetisation behaviour and specimen polarity) from sections in the Exeter Group. See Fig. 1 for location

1013 details. Symbols for specimen polarity and behaviour are larger for better quality behaviour.
1014 Ticks adjacent to logs are sampling levels. Sample numbers indicated, for data shown on other
1015 figures or in the supplementary data.
1016
1017 Fig. 5. Section logs and summary horizon magnetic polarity data for the stratigraphic section
1018 between Lympstone (site 3 on Fig. 1) to the top of the Littleham Mudstone Fm at Budleigh
1019 Salterton (Fig. 1). Bed numbers on the log for the Exmouth Mudstones and Sandstones Fm are
1020 those of Selwood *et al*. (1984). The divisions in the Littleham Mudstone Fm are from this work
1021 (detailed in the supplementary data). Ticks adjacent to logs are sampling levels. Sample numbers
1022 indicated, for data shown on other figures or in the supplementary data.
1023
1024 Fig. 6. Isothermal remanent magnetisation curves (A, C, E) and thermal demagnetisation of
1025 orthogonal isothermal remanent magnetisation (IRM) in B, D, F, for representative specimens.
1026 The Two numbers after lithology type are the magnetic susceptibility in $x10^{-5}$ SI and NRM
1027 intensity in mA/m, respectively. Specimen numbers are those shown on Figs. 4 and 5.
1028 sst=sandstone; TBF= Teignmouth Breccia Fm, EBF= Exe Breccia Fm.
1029
1030 Fig. 7. Anisotropy of magnetic susceptibility data for the Littleham Mudstone Fm (A, E, I), The
1031 Exmouth Mudstone and Sandstone Fm (B, F, J), aeolian sandstones in the Dawlish Sandstone
1032 and Teignmouth Breccia formations (C, G, K), and the various breccia units (D, H, I). A), B), C),
1033 D) are steroegraphic projections of the specimen K_{max} and K_{min} directions. E), F), G), H) are the
1034 AMS ellipsoid shape ($T= [2(L_{int}-L_{min})/(L_{max}-L_{min})]-1$; where $L=Ln(K_i)$) and strength ($P = K_{max}/K_{min}$; Tarling & Hrouda, 1993), I), J), K), L), rose diagrams showing the directions of the
1036 K_{max} axes (mirrored about 0-180 axis), indicating the preferred grain long-axis directions in the
1037 bedding plane. Ns=number of specimens.
1038
1039 Fig. 8. Representative demagnetisation data from: (A, B) the Littleham Mudstone Fm, (C, D)
1040 Exmouth Mudstone and Sandstone Fm, (E) Exe Breccia Fm, (F) Dawlish Sandstone Fm, (G)
1041 Teignmouth Breccia and (H) Watcombe Fm. A) Specimen L35, normal polarity (behaviour S1,
1042 ChRM 500-660°C), B) EM30-4, reverse polarity (behaviour T1, component A, 0-500°C), C) E20,
1043 normal polarity (behaviour S2, ChRM 600°C to origin), D) EL63, reverse polarity (behaviour T1,
1044 Component A, 0-300°C), E) EB8-1A, normal polarity (behaviour S2, ChRM 300-500°C & 540°C
1045 to origin), F) DS21-1, reverse polarity (behaviour T1, steps 500°C and above noisy due to

thermal alteration), G) DS4-2, reverse polarity (behaviour S2, ChRM 500-650°C), H) WB1-4, reverse polarity (behaviour S1, ChRM 100-620°C, 680°C step shows thermal alteration). See Figs. 4, 5 for specimen locations.

Fig. 9. a) Stereographic projection of all ChRM directions, with mean of these directions indicated for the units from the Aylesbeare Mudstone Group. B) The progressive unfolding fold test of Watson & Enkin (1993), using the data from the Exeter Group; showing the change in Fisher k with unfolding (left) and a pseudo-sampling bootstrap (right) to estimate the 95% confidence interval on the percentage unfolding.

Fig. 10. A) Detailed magnetostratigraphic data for the stratigraphic section between the Lympstone sections (3 on Fig. 1) and Littleham Cove. i) Demagnetisation behaviour showing categorisation into good (S1) and poor (S3) ChRM line-fits; great circle fit quality range from good (T1) to poor (T3), and specimens with no Triassic magnetisation are indicated in the P/X column . ii) Interpreted specimen polarity quality, with those in the greyed column not assigned a polarity. Poorest quality in column headed '??'. iii) VGP latitude, with filled symbols for those specimens possessing an S-class ChRM, and unfilled symbols for specimens with T-class, great-circle behaviour. Polarity column: white= reversed polarity, black =normal polarity, grey= uncertain, gap=X; half bar-width indicates a single useful specimen from this horizon. B) Detailed magnetostratigraphic data for the stratigraphic section between Littleham Cove and Budleigh Salterton (1 on Fig. 1). Column details as in A).

Fig. 11. Summary magnetostratigraphic data for European Permian sections, compared to the composite geomagnetic magnetic polarity timescale (GPTS) of Hounslow (submitted). Southern North Sea data for the Leman Sandstone Fm from Turner *et al*. (1999) and Lawton & Robertson (2003). Czaplinek, Piła and Jaworzna IG-1 well data based on Nawrocki (1997) and Słowakiewicz *et al*. (2009). Mirow well data from Menning *et al*. (1988) and Langereis *et al*. (2010), Schlierbachswald-4 and Everdingen 1 wells from Szurlies *et al*. (2003) and Szurlies (2013). Related Russian stages tied to the magnetostratigraphy from Hounslow (submitted). Conodont zones labelled with Guadalupian (G) and Lopingian (L) zonal codes from Jin *et al*. (2000) and Shen *et al*. (2010). Early Wuchiapingian carbon isotope excursions (CIE) and Kamura event duration from Chen *et al.* (2011), Isozaki *et al.* (2011).

1079

Type/ Location/ Unit	Dec (°)	Inc (°)	K	α95 (°)	Nl/Np	Reversal Test	G_O/G_C (°)	Plat (°)	Plong (°)	Dp/Dm (°)
Littleham Mudstone Fm										
Line fits[$]	12.4	29.2	26.0	5.4	28/0	R-	11.9/10.4*	53.6	156.3	3.3/6.0
GC means[+]	10.3	29.2	24.1	4.1	28/25	Rc	11.2/11.2	54.0	159.6	2.5/4.5
Exmouth Mudstone and Sandstone Fm										
Line fits[$]	14.0	27.1	22.2	4.3	52/0	Rc	11.3/13.3*	52.0	154.2	2.6/4.7
GC means[+]	14.2	29.0	18.2	3.8	52/27	Rb	2.4/10.0*	53.1	153.5	2.3/4.2
Dawlish Sandstone and Exe Breccia fms										
Line fits[$]	5.0	26.6	40.4	7.3	11/0	Rc	7.5/20.0	53.2	168.5	4.3/7.9
GC means[+]	359.4	32.7	8.1	11.3	11/12	Rc	9.6/11.9*	56.9	185.7	7.2/12.8
Teignmouth Breccia Fm										
GC mean[+]	174.8	-25.1	25.1	8.5	10/3	-	-	52.4	184.8	4.9/9.1
Oddicombe Breccia Fm										
Shaldon and Maidencombe[$]	191.4	-24.4	116	3.4	16/0	-	-	51.1	158.6	2.0/3.6
Watcombe Fm, basal Oddicombe Breccia										
Watcombe[$]	173.4	-20.0	28.0	10.7	8/0	-	-	49.5	186.5	5.9/11.2
Other units and data										
Knowle Sandstone[$]	195	-17	6842	3	2/0	-		-	-	-
Exeter Volc. Fm[1]	198	-25	23	6.5	23/0	-		49.5	148.5	-3.8/7.0
Exeter Volc. Fm[2]	189	-19	29	10	9/0	-		48	163	-5.4/10.4
Exeter Gp sediments[2]	188	-14	24	26	3/0	-		-	-	
Group means										
Aylesbeare Mudstone Gp	13.5	27.8	23.6	3.3	80/0	Rb	6.7/7.4*	52.5	154.9	2.0/3.6
Exeter Gp sediments	3.3	24.8	35.4	3.6	45/0	Rb	5.5/10.0*	52.4	171.2	2.1/3.9

Table 1. Directional means (with tectonic correction), reversal tests and VGP poles. [+]=great circle combined mean using method of McFadden & McElhinney (1988). [$]=conventional Fisher mean. Nl=number of specimens using with fitted lines, and Np =number of specimens with great circle planes used in the determining the mean direction. α_{95}, Fisher 95% cone of confidence. k, Fisher precision parameter. G_O is the angular separation between the inverted reverse and normal directions, and Gc is the critical value for the reversal test. In the reversal test the Go/Gc values flagged with * indicate common K values, others not flagged have statistically different K-values for reverse and normal populations, in which case a simulation reversal test was performed. Plat and Plong are the latitude and longitude of the mean virtual geomagnetic pole. [1]From Zijderveld (1967); [2] from Cornwall (1967)

Fig.1

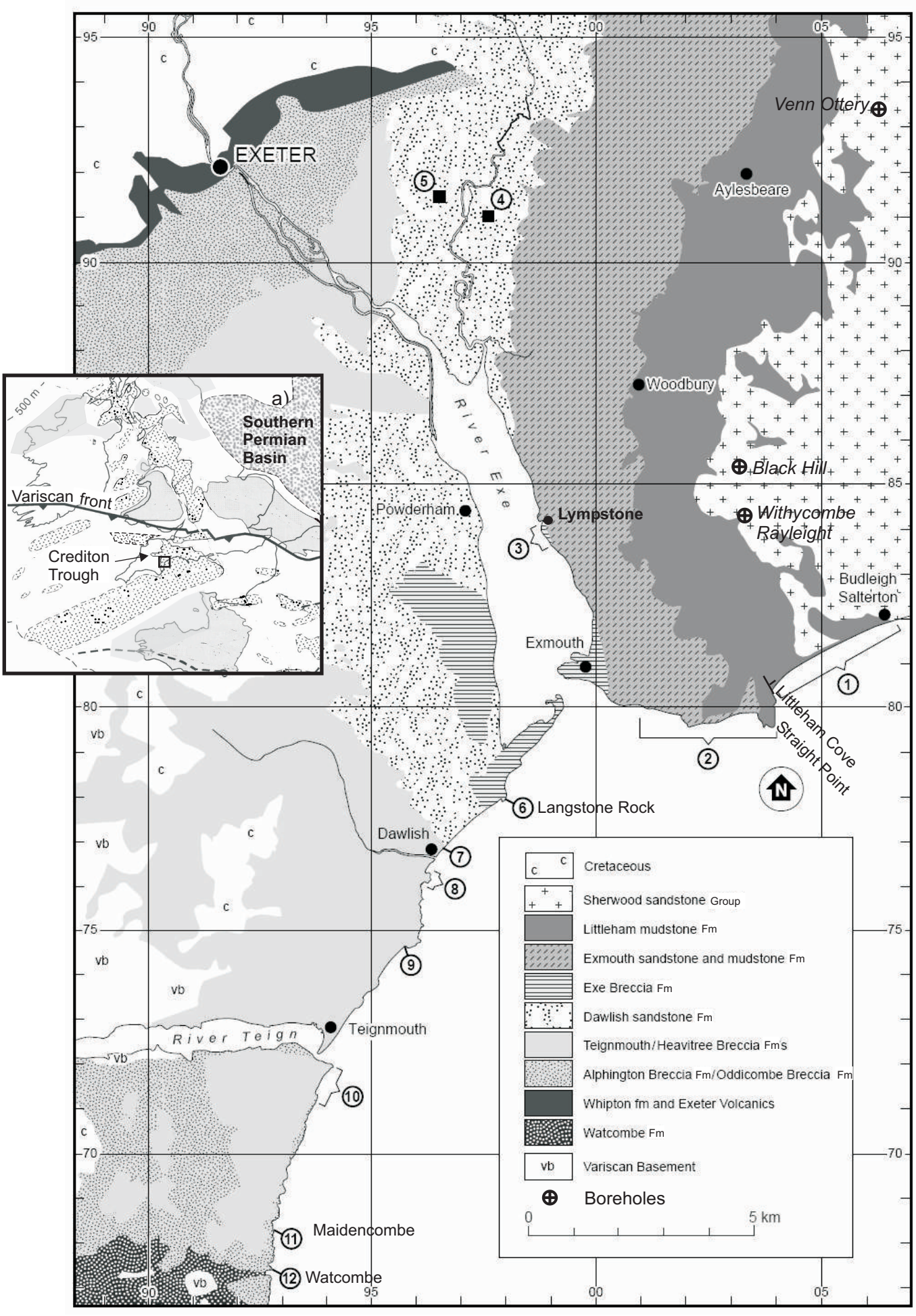
EXETER
Venn Ottery
Aylesbeare
Woodbury
Black Hill
Withycombe Rayleight
Budleigh Salterton
Lympstone
Powderham
Exmouth
Littleham Cove
Straight Point
Langstone Rock
Dawlish
Teignmouth
River Teign
River Exe
Maidencombe
Watcombe
a)
Southern Permian Basin
Variscan front
Crediton Trough
500 m
Cretaceous
Sherwood sandstone Group
Littleham mudstone Fm
Exmouth sandstone and mudstone Fm
Exe Breccia Fm
Dawlish sandstone Fm
Teignmouth/Heavitree Breccia Fm's
Alphington Breccia Fm/Oddicombe Breccia Fm
Whipton fm and Exeter Volcanics
Watcombe Fm
Variscan Basement
Boreholes
0
5 km

Fig.2

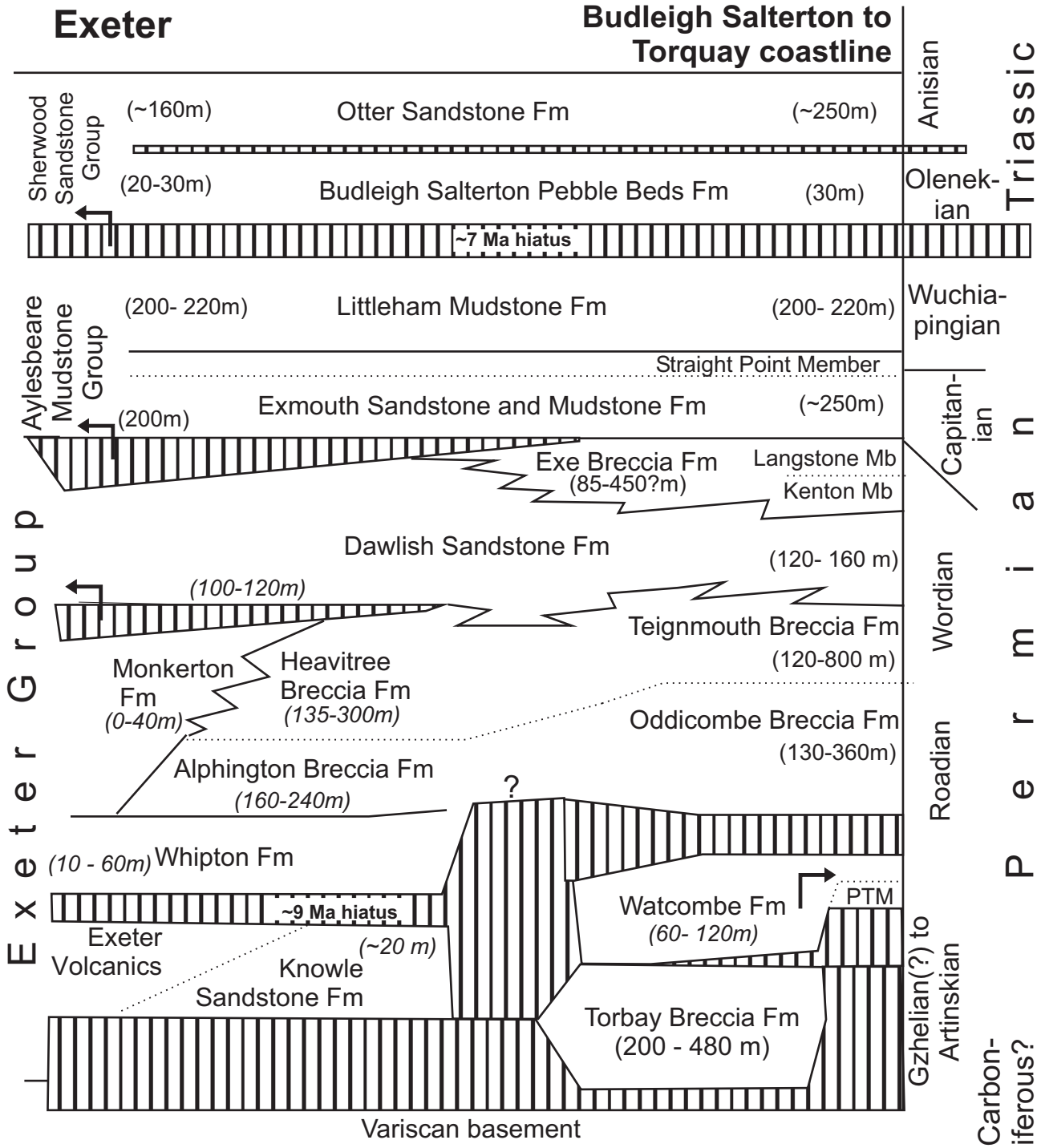
Exeter
Budleigh Salterton to Torquay coastline
Sherwood Sandstone Group
(~160m)
Otter Sandstone Fm
(~250m)
Anisian
(20-30m)
Budleigh Salterton Pebble Beds Fm
(30m)
Olenek-ian
Triassic
~7 Ma hiatus
Aylesbeare Mudstone Group
(200- 220m)
Littleham Mudstone Fm
(200- 220m)
Wuchia-pingian
Straight Point Member
Exmouth Sandstone and Mudstone Fm
(~250m)
(200m)
Capitan-ian
Exe Breccia Fm
(85-450?m)
Langstone Mb
Kenton Mb
Dawlish Sandstone Fm
(120- 160 m)
(100-120m)
Teignmouth Breccia Fm
(120-800 m)
Wordian
Monkerton Fm
(0-40m)
Heavitree Breccia Fm
(135-300m)
Oddicombe Breccia Fm
(130-360m)
Alphington Breccia Fm
(160-240m)
?
Roadian
Exeter Group
Permian
(10 - 60m)
Whipton Fm
~9 Ma hiatus
Watcombe Fm
(60- 120m)
PTM
Exeter Volcanics
(~20 m)
Knowle Sandstone Fm
Torbay Breccia Fm
(200 - 480 m)
Gzhelian(?) to Artinskian
Carbon-iferous?
Variscan basement

Fig.3

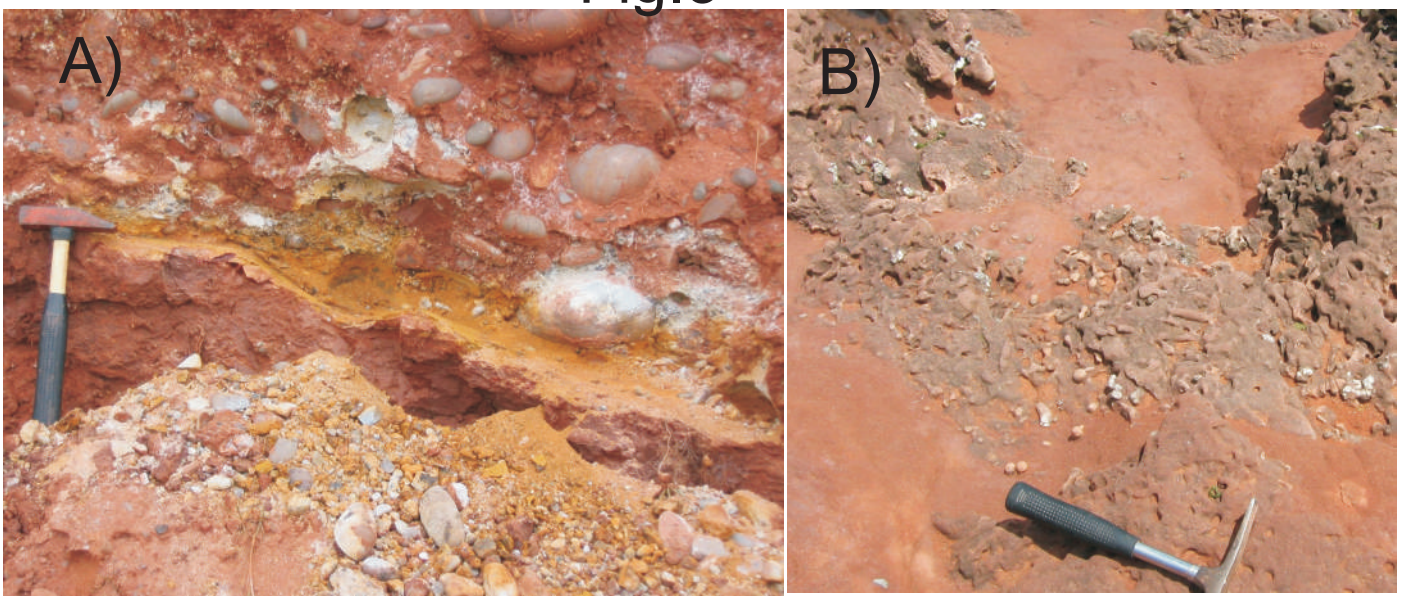

+Base Littleham Fm Breccia (Sylvie?)

+Watcombe/Oddicombe boundary (Deryck)

+Micrograph 1 (mwh)

+Micrograph 2 (mwh)

Fig.4

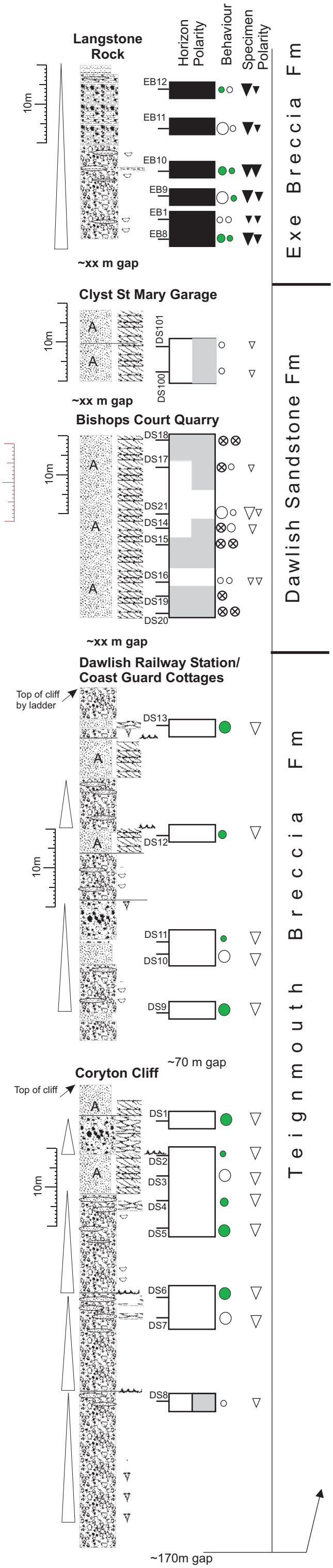
Langstone Rock
Horizon Polarity
Behaviour
Specimen Polarity
10m
EB12
EB11
EB10
EB9
EB1
EB8
~xx m gap
Clyst St Mary Garage
10m
A
A
DS101
DS100
~xx m gap
Bishops Court Quarry
10m
A
A
A
DS18
DS17
DS21
DS14
DS15
DS16
DS19
DS20
~xx m gap
Dawlish Railway Station/
Coast Guard Cottages
Top of cliff
by ladder
DS13
A
DS12
A
10m
DS11
DS10
DS9
~70 m gap
Coryton Cliff
Top of cliff
A
A
10m
DS1
DS2
DS3
DS4
DS5
DS6
DS7
DS8
~170m gap
Exe Breccia Fm
Dawlish Sandstone Fm
Teignmouth Breccia Fm
Key
Breccia
Breccia with sandstone layers
Sandstone
Siltstone/mudstone
with breccia layers
Siltstone/mudstone
Aeolian x-bedding
Fluvial x-bedding
Scoured contact
Shallow Channels
Sandstone dykes
Burrows
Fining-up
sequence
A Aeolian
Horizon Polarity
Normal Polarity
Reverse Polarity
Uncertain Polarity
Specimen Polarity
Reverse Polarity
Normal Polarity
1 2 3
Demagnetisation Behaviour
P/X
GC Fit
Line Fit
200
180
20 m
160
140
Holkham Beach
Horizon Polarity
Behaviour
Specimen Polarity
H2
H1
200-500m gap
Ness Point to Bundle Head
+30m breccia
SH2
120
SH1
100
SH3
80
SH4
SH5
60
20 m
40
SH6
20
~60 m gap
Maidencombe Beach
0
20 m
20
MB5
Cafe
40
MB2
MB1
MB3
60
MB4
Whitsand to Watcombe beachs
~70 m gap
80
20 m
100
WB5
120
140
WB6
160
180
WB3
WB2
WB1
200
Teignmouth Breccia Fm
Oddicombe Breccia Fm
Watcombe Fm

Fig.5

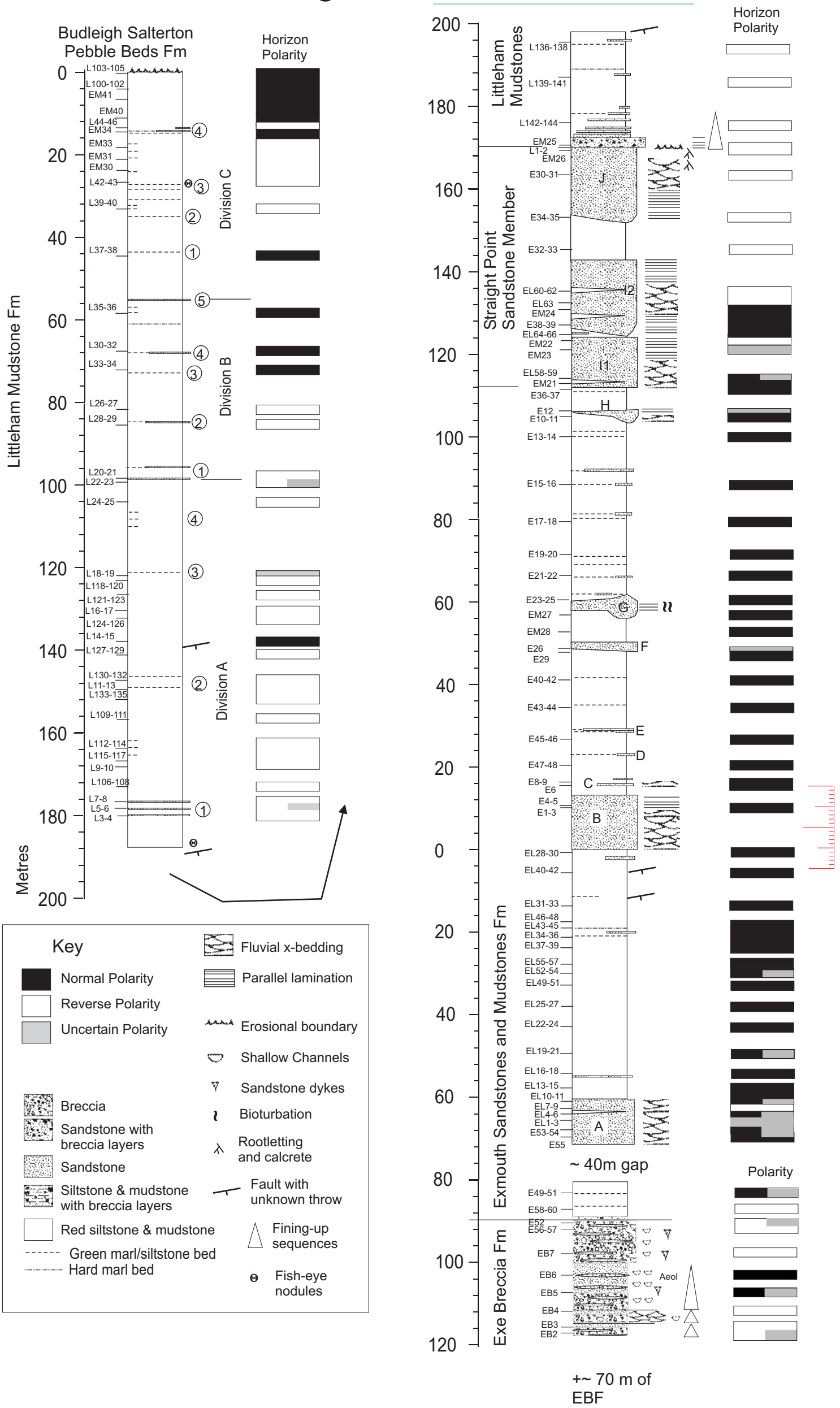
Budleigh Salterton Pebble Beds Fm
Horizon Polarity
Littleham Mudstone Fm
Metres
Division C
Division B
Division A
Littleham Mudstones
Straight Point Sandstone Member
Exmouth Sandstones and Mudstones Fm
Exe Breccia Fm
~ 40m gap
+~ 70 m of EBF
Polarity
Aeol
Key
Normal Polarity
Reverse Polarity
Uncertain Polarity
Breccia
Sandstone with breccia layers
Sandstone
Siltstone & mudstone with breccia layers
Red siltstone & mudstone
Green marl/siltstone bed
Hard marl bed
Fluvial x-bedding
Parallel lamination
Erosional boundary
Shallow Channels
Sandstone dykes
Bioturbation
Rootletting and calcrete
Fault with unknown throw
Fining-up sequences
Fish-eye nodules

Fig.6

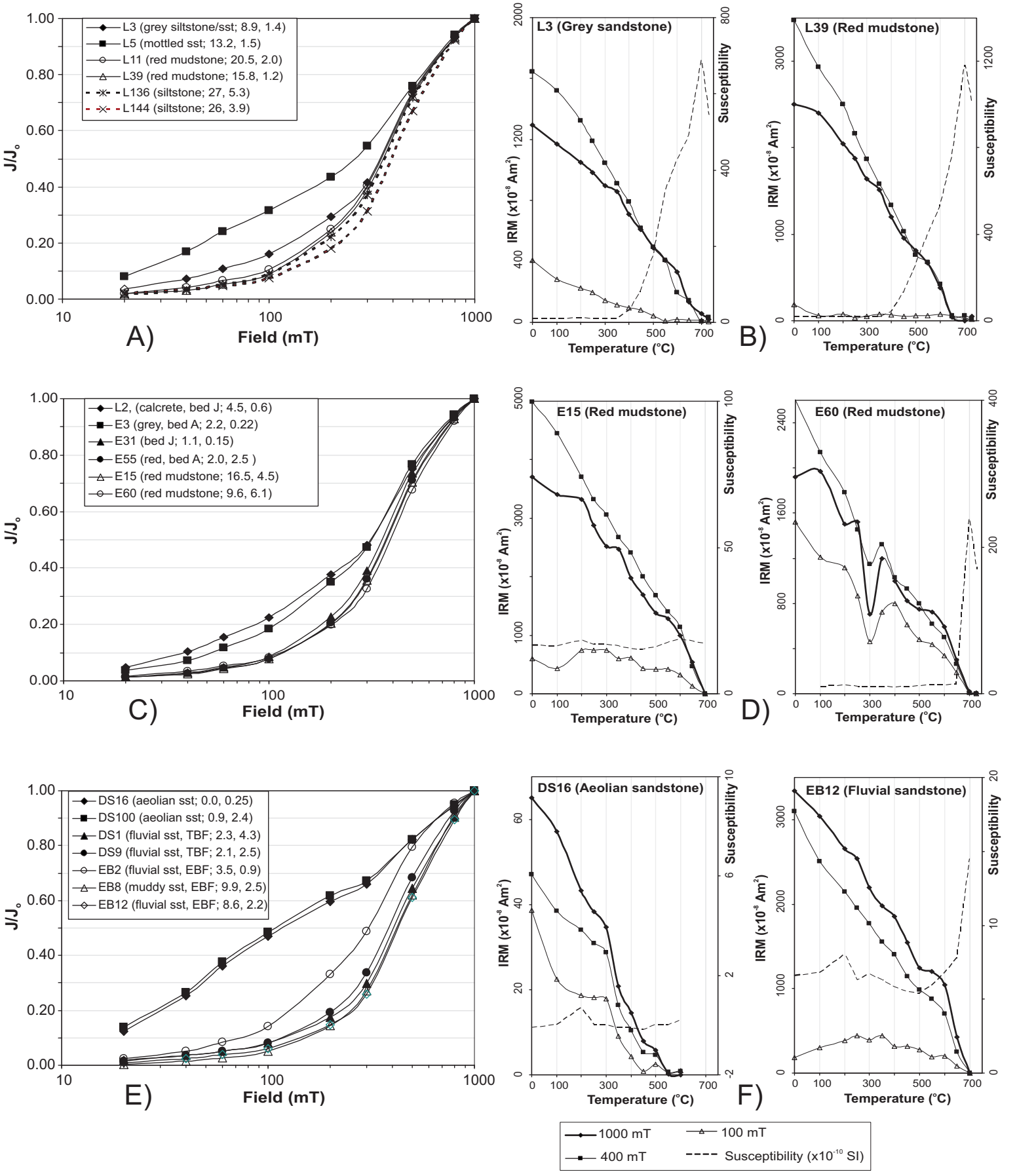
L3 (grey siltstone/sst; 8.9, 1.4)
L5 (mottled sst; 13.2, 1.5)
L11 (red mudstone; 20.5, 2.0)
L39 (red mudstone; 15.8, 1.2)
L136 (siltstone; 27, 5.3)
L144 (siltstone; 26, 3.9)
J/J$_o$
Field (mT)
A)
L3 (Grey sandstone)
L39 (Red mudstone)
IRM (x10^{-8} Am^2)
Susceptibility
Temperature (°C)
B)
L2, (calcrete, bed J; 4.5, 0.6)
E3 (grey, bed A; 2.2, 0.22)
E31 (bed J; 1.1, 0.15)
E55 (red, bed A; 2.0, 2.5)
E15 (red mudstone; 16.5, 4.5)
E60 (red mudstone; 9.6, 6.1)
C)
E15 (Red mudstone)
E60 (Red mudstone)
D)
DS16 (aeolian sst; 0.0, 0.25)
DS100 (aeolian sst; 0.9, 2.4)
DS1 (fluvial sst, TBF; 2.3, 4.3)
DS9 (fluvial sst, TBF; 2.1, 2.5)
EB2 (fluvial sst, EBF; 3.5, 0.9)
EB8 (muddy sst, EBF; 9.9, 2.5)
EB12 (fluvial sst, EBF; 8.6, 2.2)
E)
DS16 (Aeolian sandstone)
EB12 (Fluvial sandstone)
F)
1000 mT
400 mT
100 mT
Susceptibility (x10^{-10} SI)

Fig.7

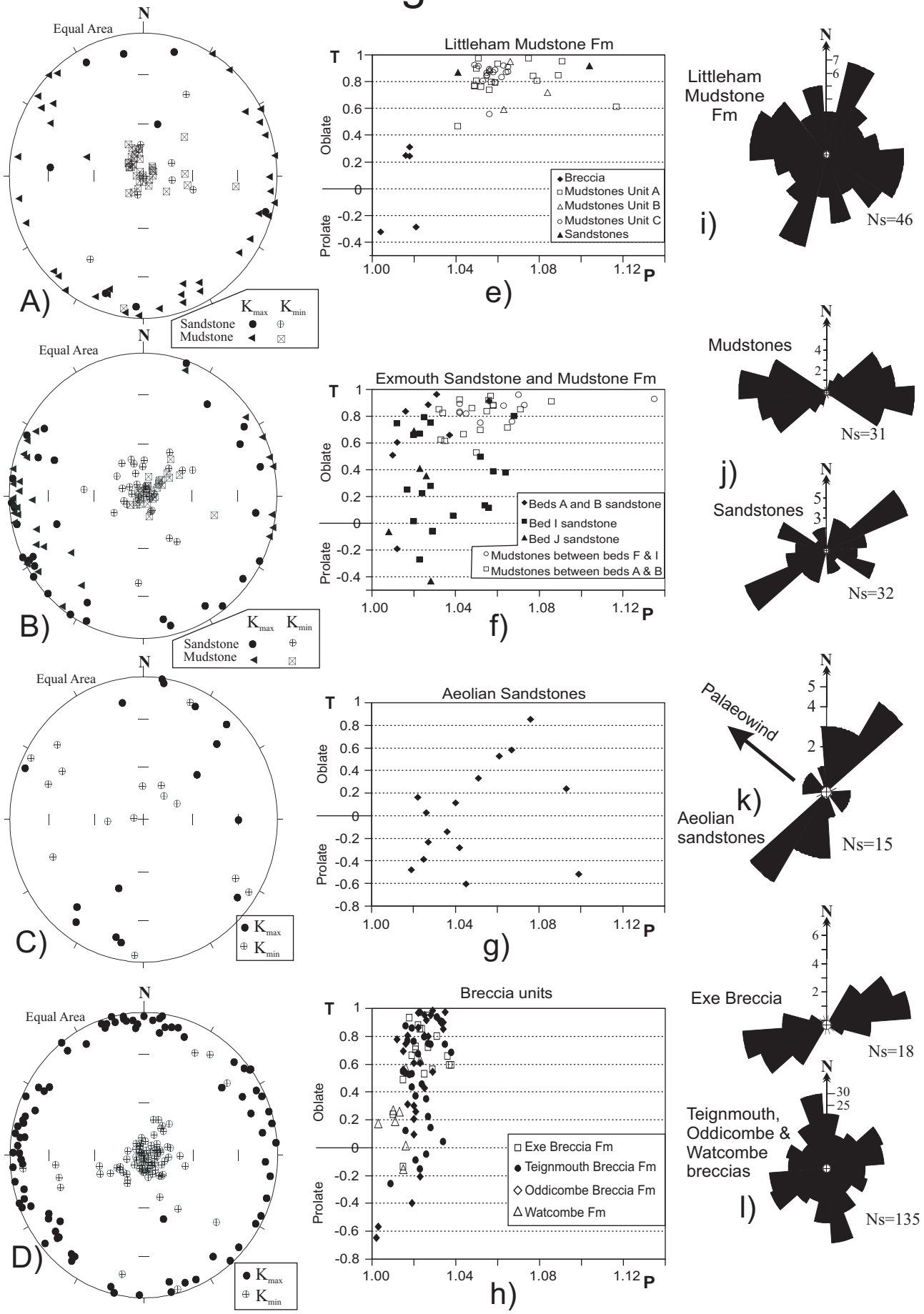
N
Equal Area
A)
K_{max} K_{min}
Sandstone
Mudstone
B)
C)
D)
Littleham Mudstone Fm
T
Oblate
Prolate
Breccia
Mudstones Unit A
Mudstones Unit B
Mudstones Unit C
Sandstones
P
e)
Exmouth Sandstone and Mudstone Fm
Beds A and B sandstone
Bed I sandstone
Bed J sandstone
Mudstones between beds F & I
Mudstones between beds A & B
f)
Aeolian Sandstones
g)
Breccia units
Exe Breccia Fm
Teignmouth Breccia Fm
Oddicombe Breccia Fm
Watcombe Fm
h)
Littleham Mudstone Fm
i)
Ns=46
Mudstones
Ns=31
j)
Sandstones
Ns=32
Palaeowind
k)
Aeolian sandstones
Ns=15
Exe Breccia
Ns=18
Teignmouth, Oddicombe & Watcombe breccias
l)
Ns=135

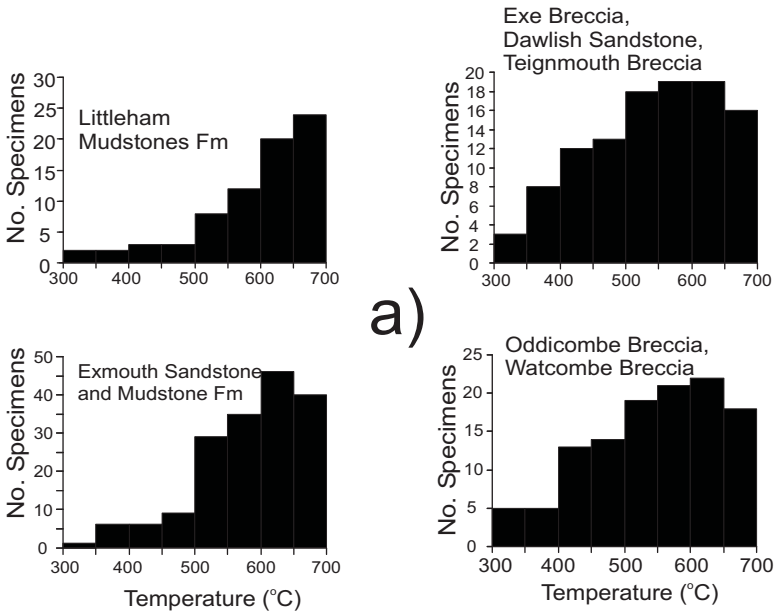

b)

	Class	Ns	95	
Aylesbeare Mudstone Group	S1	23	5.7	2.1
	S2	28	10.6	2.4
	S3	29	13.9	3.2
	T1	21	18.1	2.9
	T2	21	20.7	2.2
	T3	24	19.8	2.9
Exeter Group	S1	31	3.2	2.9
	S2	5	5	2.9
	S3	8	9.6	3.8
	T1	7	17.3	3.2
	T2	2	8.5	2.5
	T3	13	16.5	4.0

Fig.9

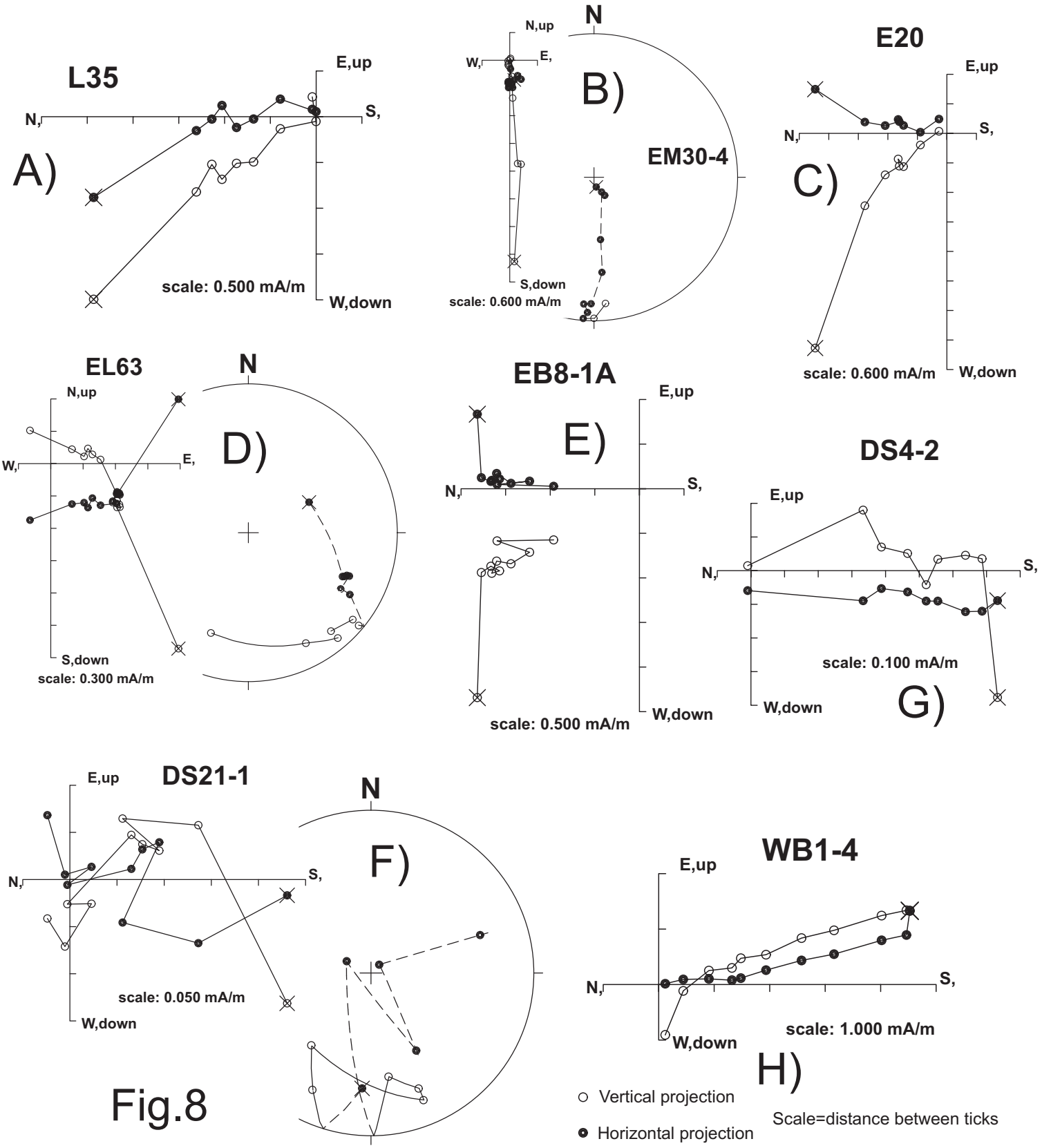
L35
A)
E,up
N,
S,
W,down
scale: 0.500 mA/m
N,up
W,
E,
S,down
scale: 0.600 mA/m
N
B)
EM30-4
E20
C)
E,up
N,
S,
W,down
scale: 0.600 mA/m
EL63
N,up
W,
E,
S,down
scale: 0.300 mA/m
N
D)
EB8-1A
E)
E,up
N,
S,
W,down
scale: 0.500 mA/m
DS4-2
E,up
N,
S,
W,down
scale: 0.100 mA/m
G)
DS21-1
E,up
N,
S,
W,down
scale: 0.050 mA/m
N
F)
WB1-4
E,up
N,
S,
W,down
scale: 1.000 mA/m
H)
Vertical projection
Horizontal projection
Scale=distance between ticks

Fig.8

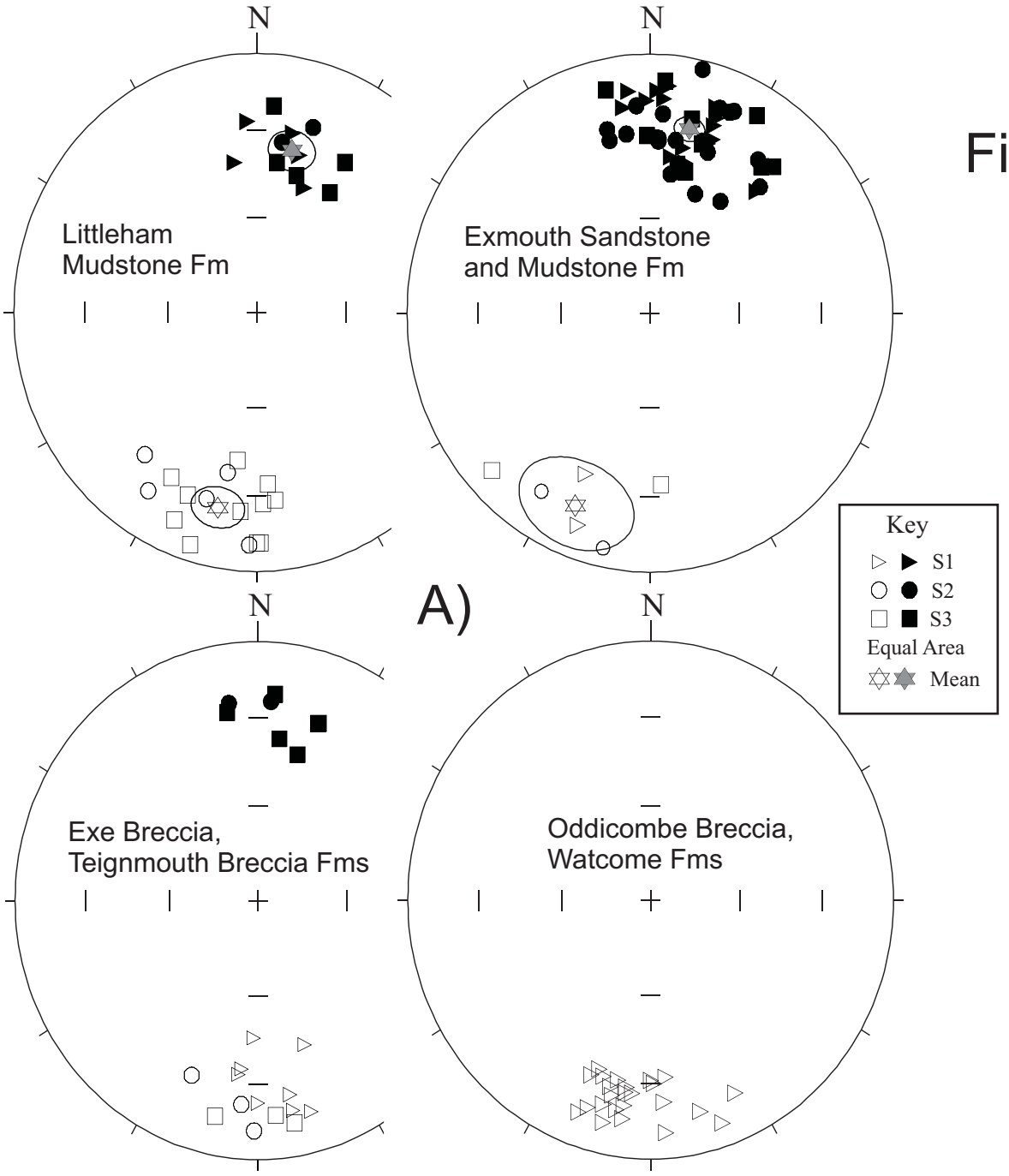
N
N
Littleham
Mudstone Fm
Exmouth Sandstone
and Mudstone Fm
A)
Key
S1
S2
S3
Equal Area
Mean
N
N
Exe Breccia,
Teignmouth Breccia Fms
Oddicombe Breccia,
Watcome Fms

Fig.10

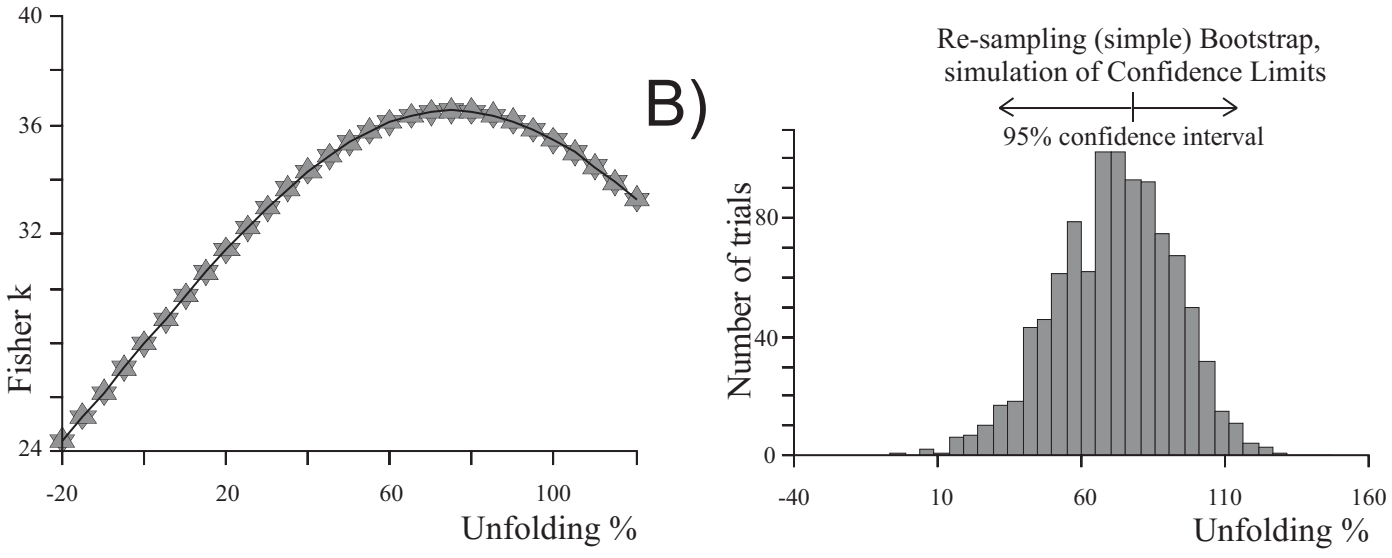
B)
40
36
32
24
Fisher k
-20
20
60
100
Unfolding %
Re-sampling (simple) Bootstrap,
simulation of Confidence Limits
95% confidence interval
Number of trials
80
40
0
-40
10
60
110
160
Unfolding %

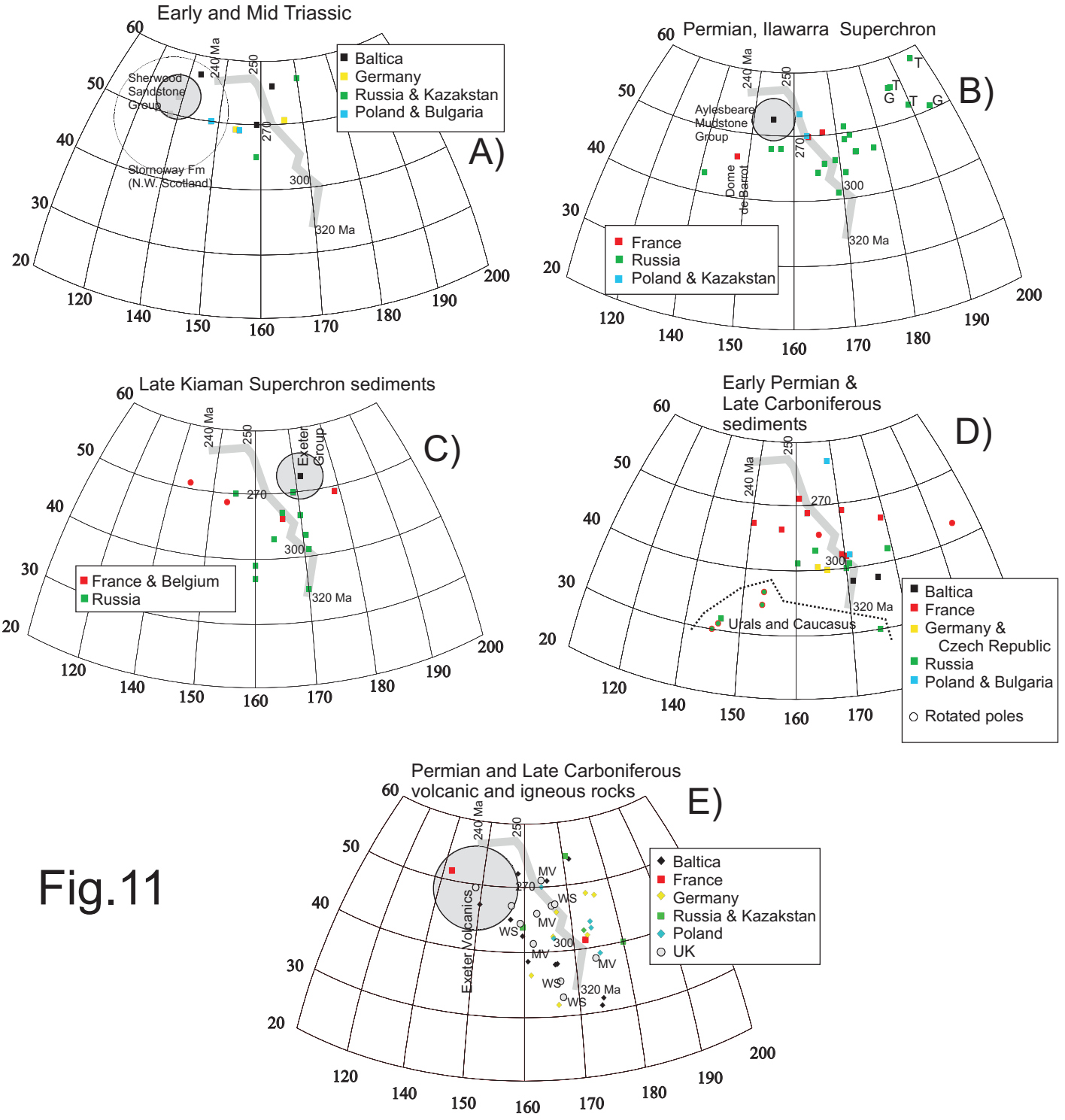
Early and Mid Triassic
A)
Sherwood Sandstone Group
Stornoway Fm (N.W. Scotland)
240 Ma
250
270
300
320 Ma
Baltica
Germany
Russia & Kazakstan
Poland & Bulgaria
Permian, Ilawarra Superchron
B)
Aylesbeare Mudstone Group
Dome de Barrot
T
G
France
Russia
Poland & Kazakstan
Late Kiaman Superchron sediments
C)
Exeter Group
France & Belgium
Russia
Early Permian & Late Carboniferous sediments
D)
Urals and Caucasus
Baltica
France
Germany & Czech Republic
Russia
Poland & Bulgaria
Rotated poles
Permian and Late Carboniferous volcanic and igneous rocks
E)
Exeter Volcanics
MV
WS
Baltica
France
Germany
Russia & Kazakstan
Poland
UK
60
50
40
30
20
120
140
150
160
170
180
190
200

Fig.11

Fig.12

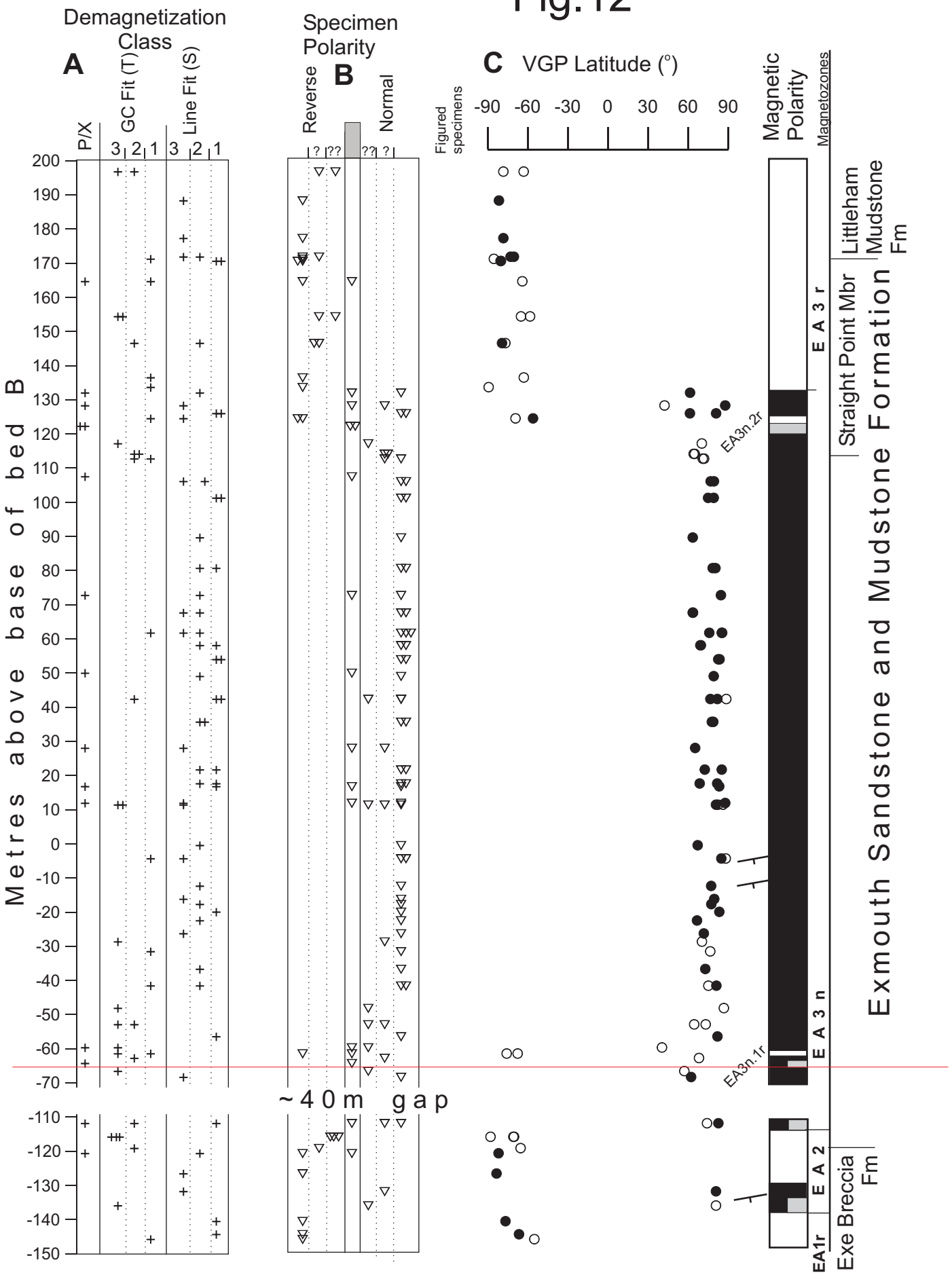
Demagnetization Class
A
P/X
GC Fit (T)
Line Fit (S)
3 2 1 3 2 1
Specimen Polarity
B
Reverse
Normal
? ?? ?? ?
C VGP Latitude (°)
-90 -60 -30 0 30 60 90
Figured specimens
Magnetic Polarity
Magnetozones
Metres above base of bed B
200 190 180 170 160 150 140 130 120 110 100 90 80 70 60 50 40 30 20 10 0 -10 -20 -30 -40 -50 -60 -70
~40m gap
-110 -120 -130 -140 -150
EA3n.2r
EA3n.1r
E A 3 r
E A 3 n
E A 2
EA1r
Littleham Mudstone Fm
Straight Point Mbr
Exmouth Sandstone and Mudstone Formation
Exe Breccia Fm

Fig.13

Demagnetization Class
A
P/X
GC Fit (T)
Line Fit (S)
3 2 1 3 2 1
Specimen Polarity
B
Reverse
Normal
? ?? ?? ?
Figured specimens
C
VGP Latitude (°)
-90 -60 -30 0 30 60 90
Magnetic Polarity
Magnetozones
BSPB Fm
Metres below BSPB Fm
0 10 20 30 40 50 60 70 80 90 100 110 120 130 140 150 160 170 180
EA5n.1r
EA3r.1n
EA 5 n
EA 4 r
EA 4 n
EA 3 r
Division C
Division B
Division A
Littleham Mudstones Formation

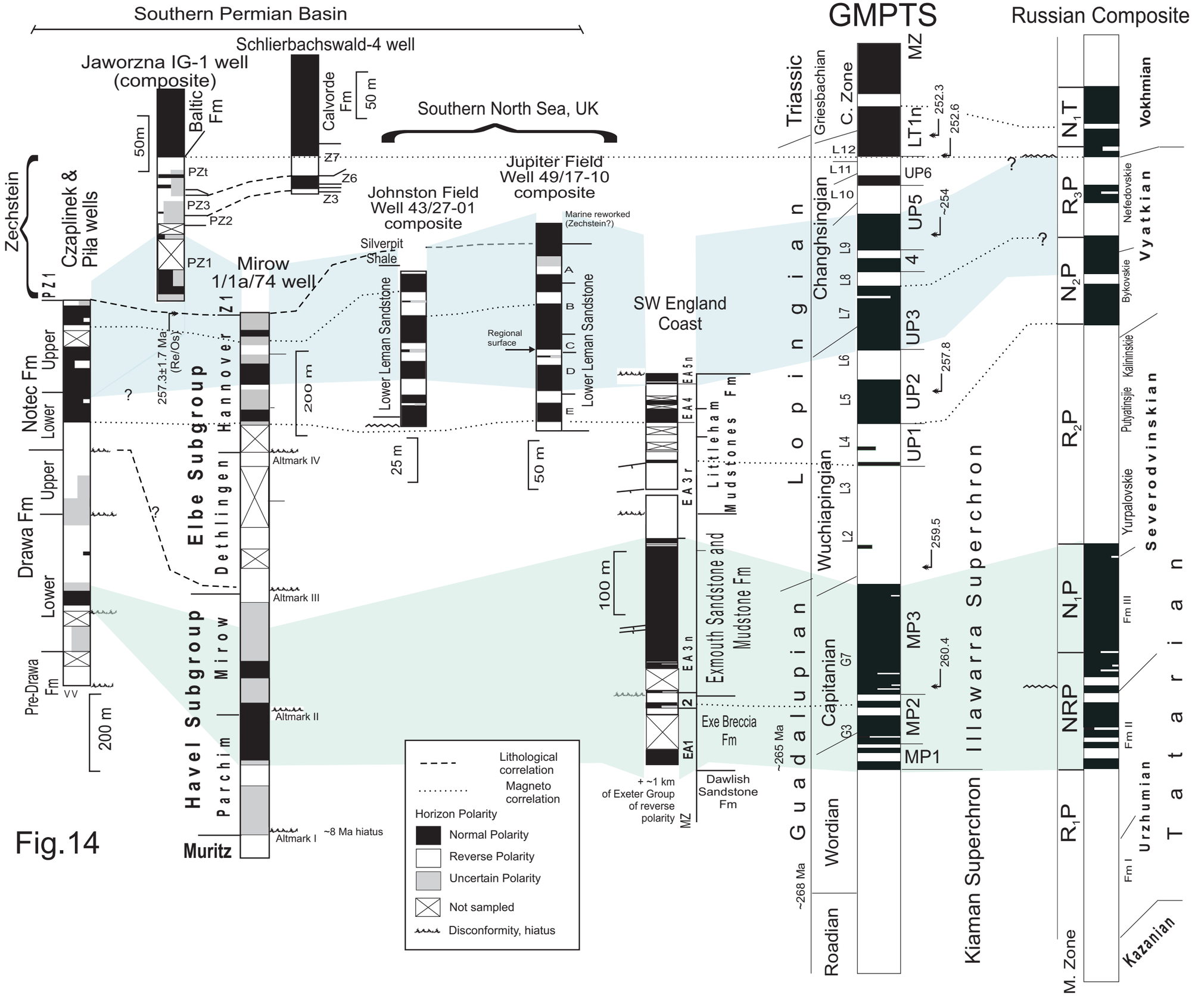
Southern Permian Basin
Schlierbachswald-4 well
Jaworzna IG-1 well (composite)
Baltic Fm
Calvorde Fm
50 m
50m
Southern North Sea, UK
Zechstein
Czaplinek & Piła wells
PZ1
PZt
PZ3
PZ2
Z7
Z6
Z3
Jupiter Field Well 49/17-10 composite
Johnston Field Well 43/27-01 composite
Marine reworked (Zechstein?)
Silverpit Shale
Mirow 1/1a/74 well
Lower Leman Sandstone
Regional surface
A
B
C
D
E
SW England Coast
Notec Fm
Upper
Lower
Z1
257.3±1.7 Ma (Re/Os)
200 m
25 m
50 m
Elbe Subgroup
Hannover
Dethlingen
Altmark IV
Altmark III
Altmark II
Altmark I
~8 Ma hiatus
Havel Subgroup
Mirow
Parchim
Muritz
Drawa Fm
Upper
Lower
Pre-Drawa Fm
200 m
EA5n
EA4
EA3r
EA3n
EA2
EA1
Littleham Mudstones Fm
Exmouth Sandstone and Mudstone Fm
100 m
Exe Breccia Fm
Dawlish Sandstone Fm
MZ
+ ~1 km of Exeter Group of reverse polarity
Lithological correlation
Magneto correlation
Horizon Polarity
Normal Polarity
Reverse Polarity
Uncertain Polarity
Not sampled
Disconformity, hiatus
GMPTS
Russian Composite
Triassic
Griesbachian
C. Zone
MZ
L12
L11
L10
L9
L8
L7
L6
L5
L4
L3
L2
LT1n
252.3
252.6
UP6
UP5
~254
4
UP3
UP2
257.8
UP1
259.5
MP3
260.4
MP2
MP1
Changhsingian
Wuchiapingian
Capitanian
G7
G3
Wordian
Roadian
~265 Ma
~268 Ma
Guadalupian
Lopingian
Kiaman Superchron
Illawarra Superchron
Tatarian
Kazanian
Urzhumian
Severodvinskian
Vyatkian
Vokhmian
N1T
R3P
N2P
R2P
NRP
N1P
R1P
M. Zone
Nefedovskie
Bykovskie
Putyatinsjie
Kalininskie
Yurpalovskie
Fm III
Fm II
Fm I

Fig.14

End of the Kiaman Superchron in the Permian of SW England: Magnetostratigraphy of the Aylesbeare Mudstone and Exeter groups.

Mark W. Hounslow, Gregg McIntosh, Richard A. Edwards, Deryck Laming, Vassil Karloukovski

Supplementary Data

The data here is composed of:

Section	No. on Fig 1	Grid ref	Lat/long	Bedding strike/dip	N_H	J_0 ($x10^{-3}$ A/m)	K_{lf} ($x10^{-5}$ SI)	Formation/unit
Budleigh Salterton to Littleham Cove	1	SY040802 to SY063817	50.622N: -3.342W	302/5	38	3.2	2.1	Littleham Mudstone Fm (LMF)
Straight Point to Maer	2	SY040802 to SY011799	50.608N: -3.376W	340/5 to 013/8	60	4.0	1.35	Exmouth Mudstone and Sandstone Fm (EMSF), base of LMF
Sowden Lane to Lympstone Harbour	3	SX990836 to SX988842	50.638N: -3.441W	321/9 to 315/8	10	2.1	3.3	Base of EMSF, top of Exe Breccia Fm
Clyst St Mary Garage	4	SX976910	50.710N: -3.454W	045/5	2	2.4	0.68	Dawlish Sandstone Fm
Bishops Court Quarry	5	SX965915	50.711N: -3.465W	045/5	6	0.74	0.57	Dawlish Sandstone Fm
Langstone Rock	6	SX980779	50.598N: -3.445W	293/8	6	2.8	7.6	Exe Breccia Fm
Dawlish Station	7	SX964767	50.580N: -3.465W	293/10	5	1.4	2.7	Teignmouth Breccia Fm
Coryton Cliff and Cove	8	SX962762	50.577N: -3.468W	319/10	8	1.5	1.9	Teignmouth Breccia Fm
Holcombe Beach	9	SX957746	50.562N:-3.475W	342/12	2	2.4	5.1	Teignmouth Breccia Fm
Ness Point to Bundle Head	10	SX941720 to SX937712	50.533N: -3.500W	355/0 to 295/5	6	7.2	9.8	Oddicombe Breccia Fm
Maidencombe Beach	11	SX928684	50.505: -3.514	275/10 to 346/6	5	9.3	7.0	Oddicombe Breccia Fm
Whitsand to Watcombe Beachs	12	SX927674	50.496: -3.515	315/41 to 288/25	5	5.8	6.4	Watcombe Fm and Oddicombe Breccia Fm
West Sandford	Not on Fig. 1	SS811027	50.812N: -3.689W	105/14	1	10.8	12.1	Knowle Sandstone Fm

Table. s1. Section and site details sampled, and average magnetic properties of the samples. NH number of sampled horizons, Jo= Initial natural remanent magnetisation intensity, klf= low frequency magnetic susceptibility. Most samples were collected from the sea cliffs, with those from Bishops Court Quarry from a working quarry (Table s1). Those from Dawlish Station and West Sandford were from small cuttings. Samples from below bed B to the base of bed A (Fig. 5), in the Exmouth Mudstone and Sandstone Fm, were from foreshore exposures and sea-cliffs, east of Exmouth. In the breccia units, suitable units for palaeomagnetic sampling were thin, discontinuous sandstone and mudstone beds.

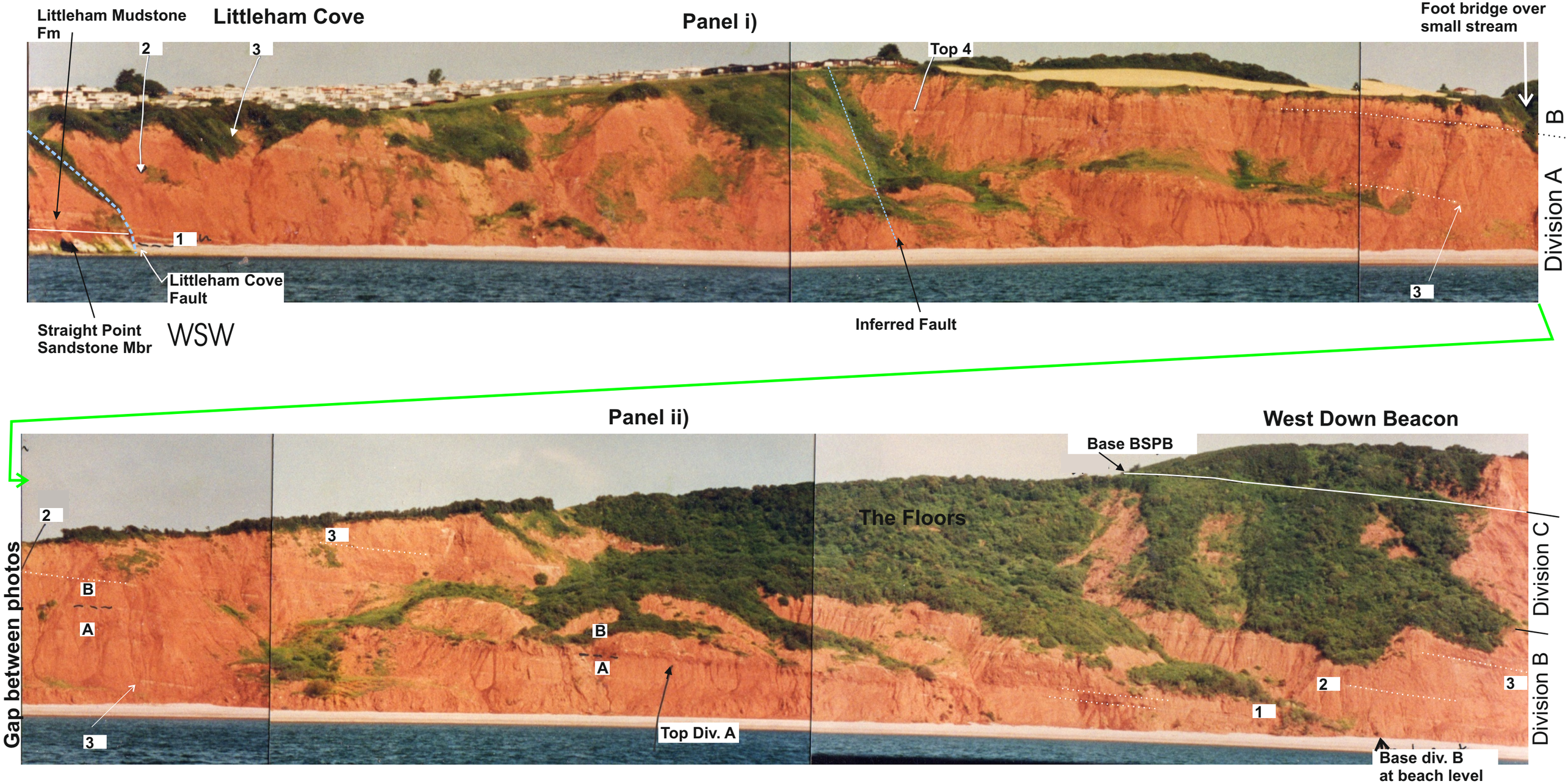

Fig.s1. Annotated photos of the cliff between Littleham Cove (panel i) and Budleigh Salterton (panel iv), indicating the bed and division sub-division of the Littleham Mudstones Formation. The three sub-divisions are a lower division A, mid division B, and an upper division C. The oldest part of the division A is exposed on the west side of the Littleham Cove fault. The W-E correlation across the Littleham Cove fault is not entirely clear, but the three sandstone beds (bed -1 in division A) may correlate to the upper-most units exposed west of the fault in the cliff adjacent to the path down the cliff. The succession is interrupted by a number of small landslips, which make the stratigraphy difficult to follow at beach level, without the photographs. The full succession can be examined by using the headwall scars behind the landslips.

Panel iii)

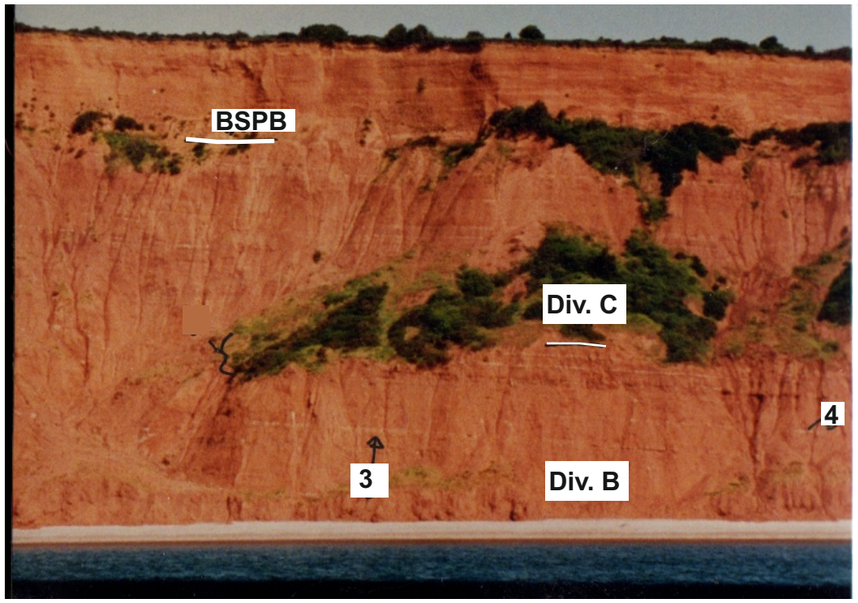

Gap between photos

Interval with many paler beds

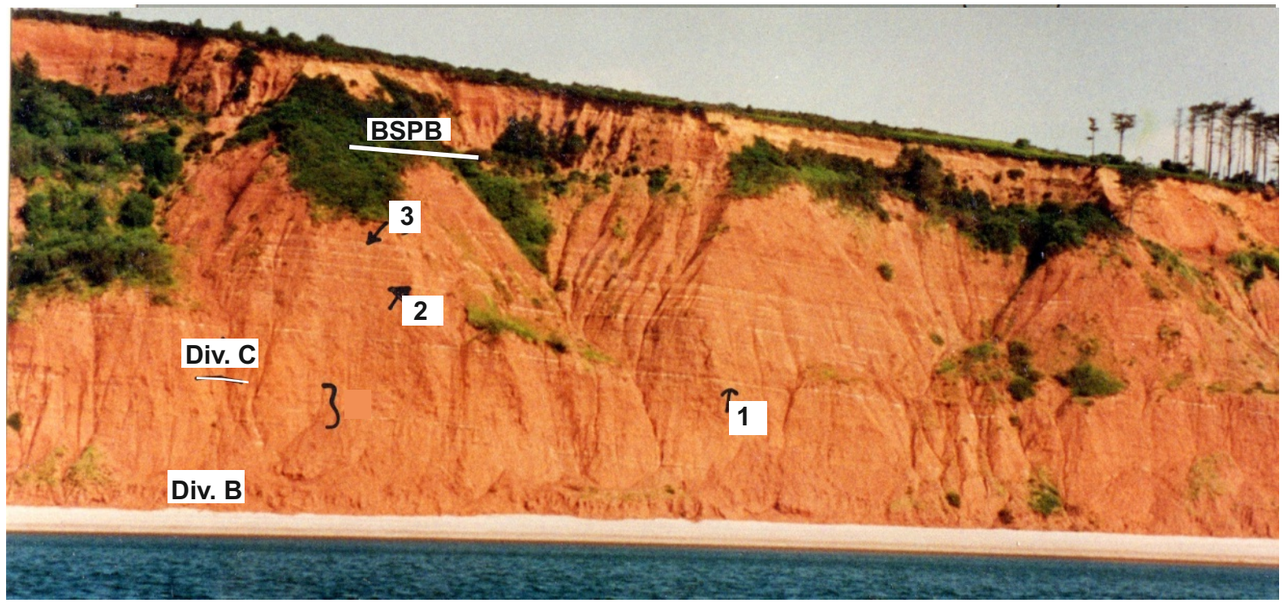

Panel iv)

ENE

Gap between photos

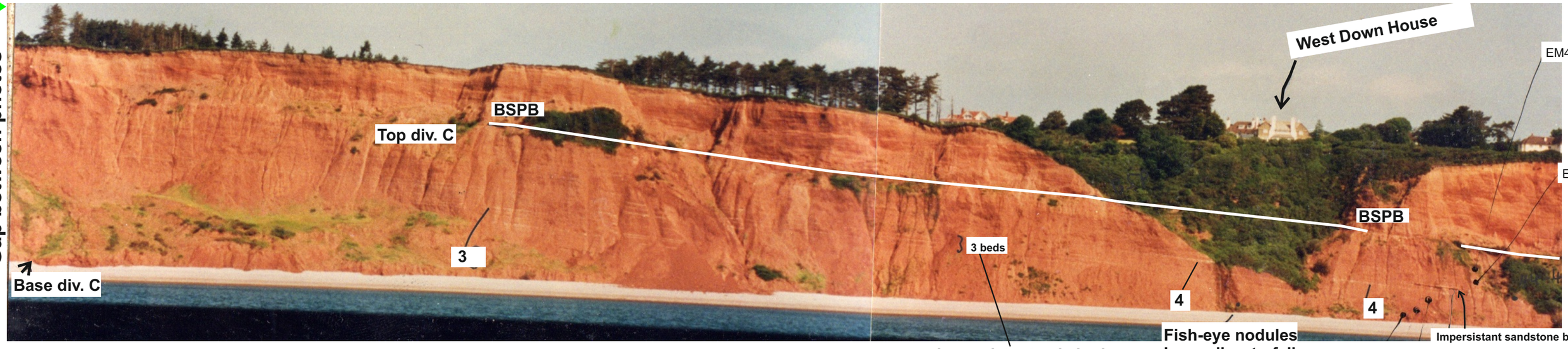

Fig.s1. Panels iii) and iv)

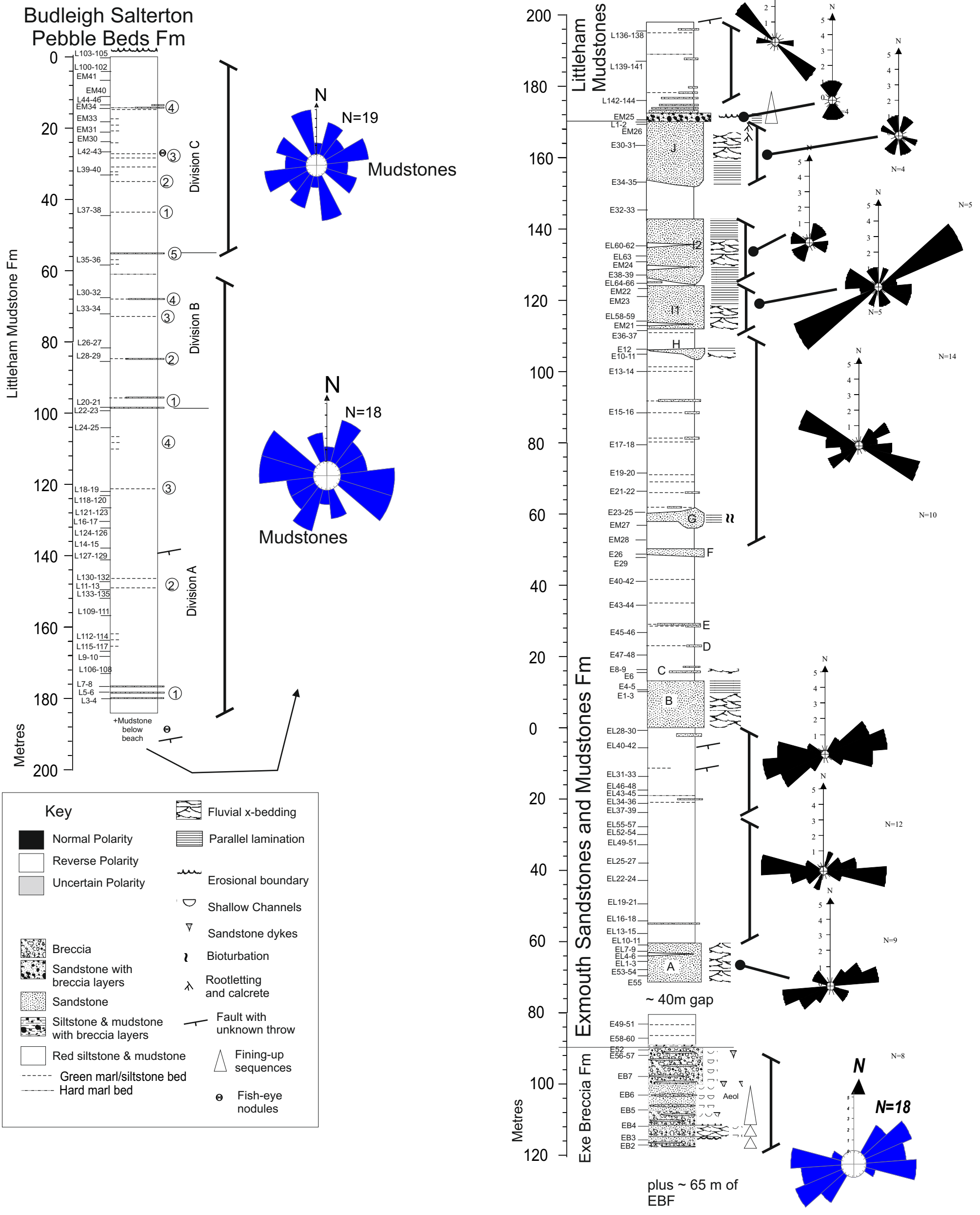

Fig.s2. K_{max} axis directions for samples from the Aylesbeare Mudstone Group. The directions have been mirrored about the 0-180 axis. The K_{max} axes directions illustrate the similarity in ENE or easterly flow directions between the Exe Breccia and the lower part of the Exmouth Mudstone and Sandstone Fm. The directions in the upper part of the Group are more variable, but likely indicate a more NE direction of sediment transport. The SE-NW Kmax axes trends seen in the mudstones above bed G, and particularly in the Littleham Mudstones Fm may represent NW directed wind transport of the clay and silt in these units.

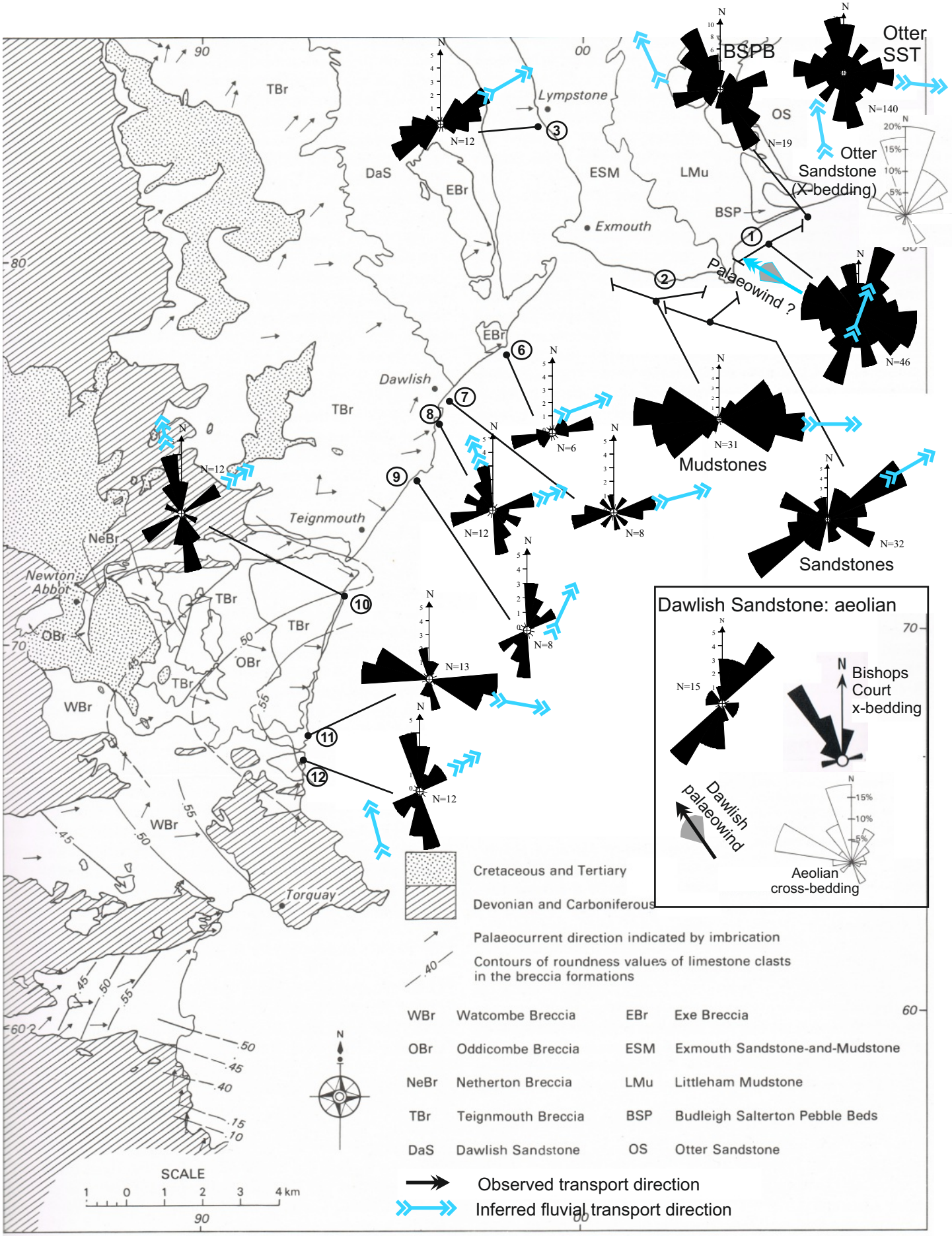

Fig.s3. Summary of transport directions and K_{max} axis directions for samples from the entire Permian, and Triassic successions west of Budleigh Salterton. Inset shows data for aeolian units, from the Dawlish Sandstone Fm (from Jones 1992, Selwood *et al.* 1984). The Kmax directions have been mirrored about the 0-180° axis (fluvial transport data from Laming 1966; Henson 1971; Selwood *et al.* 1984; Smith & Edwards 1991). The Triassic AMS data (Otter Sandstone, Budleigh Salterton Pebble Beds, BSPB) is from the samples described by Hounslow & McIntosh (2003). The Exeter Group below the Dawlish Sandstone Fm typically has bi-modal groups inferred to display ENE to easterly fluvial transport and northerly transport. Its possible in some of the sandstone and mudstones, the northerly trend may be a wind-transport direction, like seen in the aeolian units in the Dawlish Sandstone. Fluvial units in and above the Dawlish Sandstone Fm into the lower Aylesbeare Mudstone Group, show strong ENE to easterly fluvial transport. In the Littleham Mudstone Fm directions may be transitional to the northerly transport clearly seen in the overlying BSPB and Otter Sandstone.

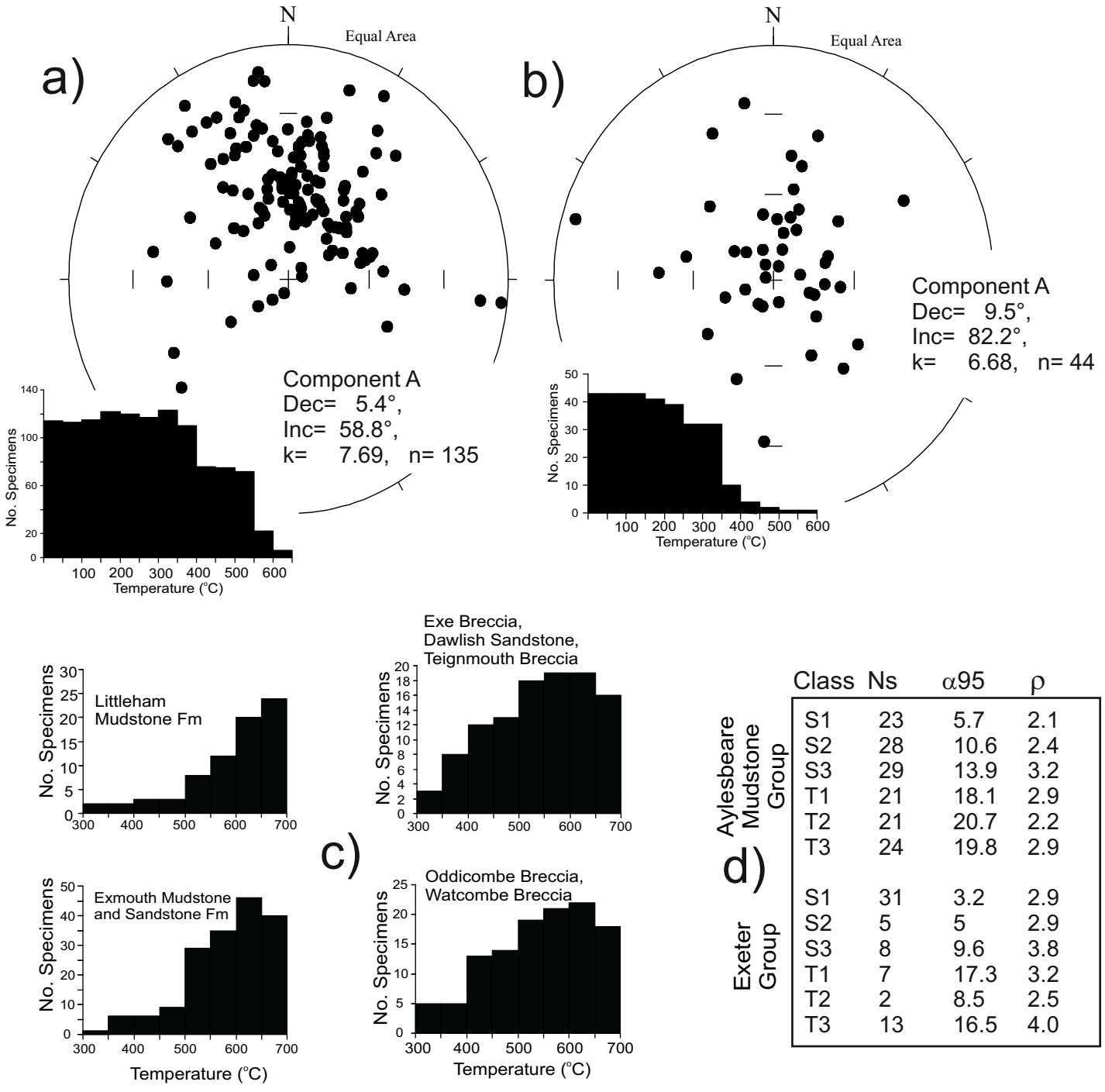

d)

	Class	Ns	α95	ρ
Aylesbeare Mudstone Group	S1	23	5.7	2.1
	S2	28	10.6	2.4
	S3	29	13.9	3.2
	T1	21	18.1	2.9
	T2	21	20.7	2.2
	T3	24	19.8	2.9
Exeter Group	S1	31	3.2	2.9
	S2	5	5	2.9
	S3	8	9.6	3.8
	T1	7	17.3	3.2
	T2	2	8.5	2.5
	T3	13	16.5	4.0

Fig.s4. Cumulative unblocking spectra for, a), b) the component A directions, from a) the Aylesbeare Mudstone Group, b) Exeter Group. C) The characteristic remanence ranges divided into stratigraphic groups. D) Statistics relating to the demagnetisation class, the number of specimens (Ns), the average α_{95} of the line (S-class) or plane (T-class) principle component fits, and the average excess standard deviation (ρ).

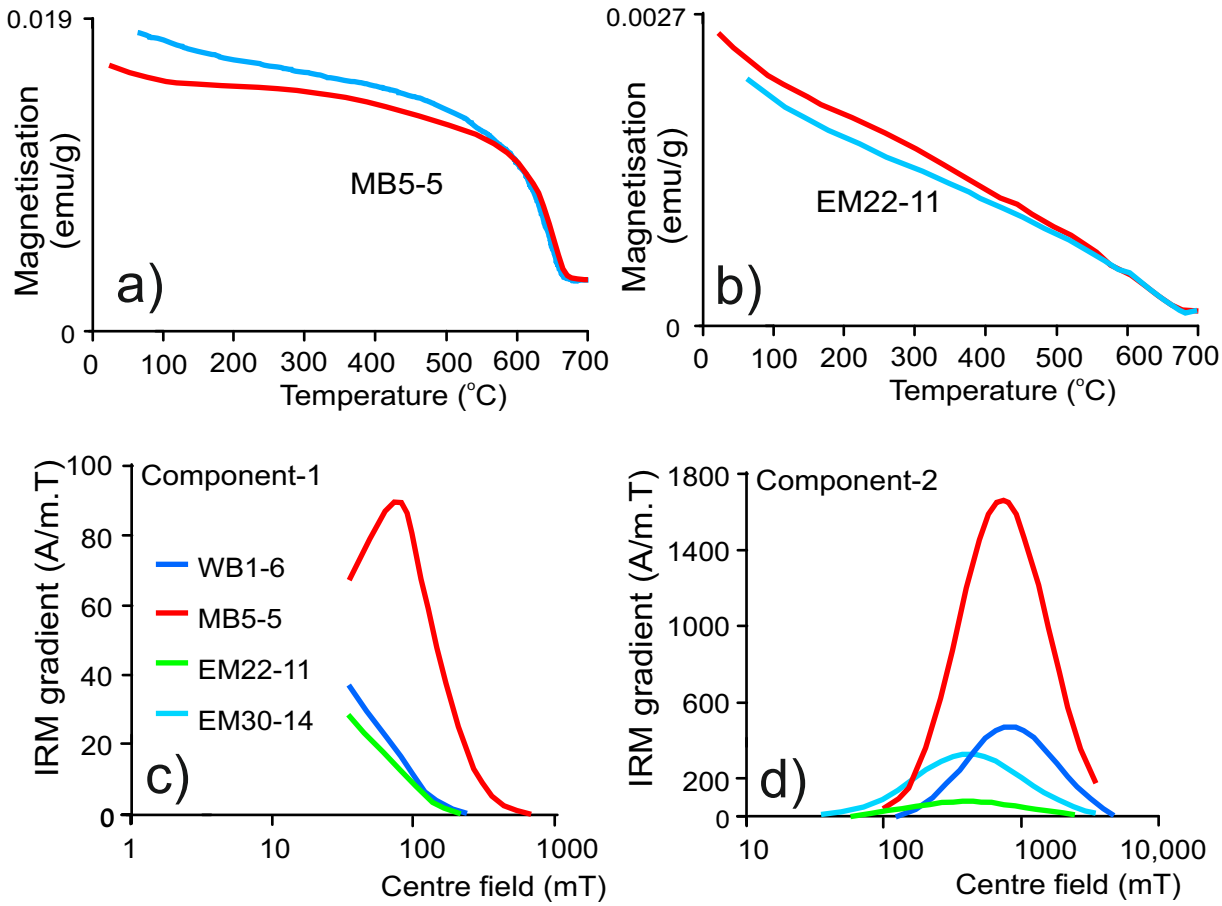

Fig.s5. A,b) Representative thermomagnetic data, measured using the vertical field translation balance (red=heating, blue= cooling). A subtle change in slope is seen at temperatures less than 200°C, which disappears when the estimated paramagnetic contribution is subtracted from the curves. C), d) log-Gaussian isothermal remanent magnetisation coercivity distributions (Kruiver *et al.* 2001) for selected samples, showing the fitted low field (component-1, c)) and high field components (component 2, d)). IRM data obtained with backfield data. Specimen WB1-6 and MB5-5 have higher coercivities (Bcr* of 741-851 and 63 mT for the 2 components) than EM22-11 and EM30-14 (Bcr* of 407-417 and 32 mT). Furthermore, these former 2 specimens had wider high coercivity distributions (dispersion parameter of 0.40-0.45 as compared to 0.32 for EM22-11 and EM30-14).

Fig.s6. Petromagnetic data for the Exeter and Aylesbeare Mudstone groups. Sandstone samples in blue, mudstone samples in red, and sandstone & sandy-mudstone units from breccia units in green.

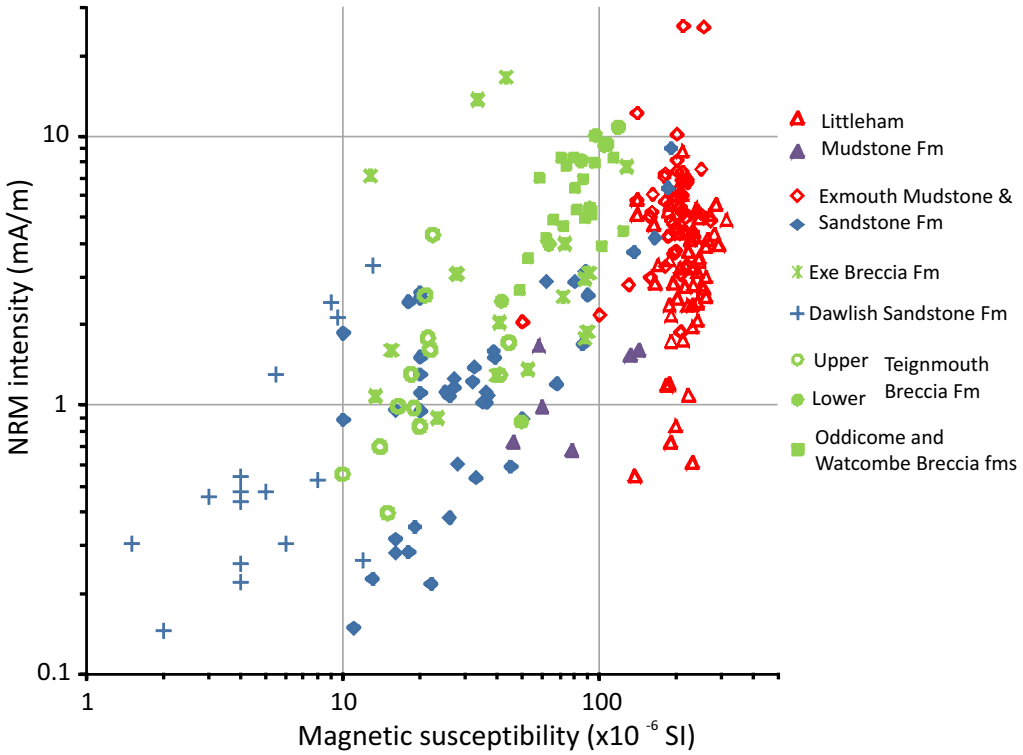

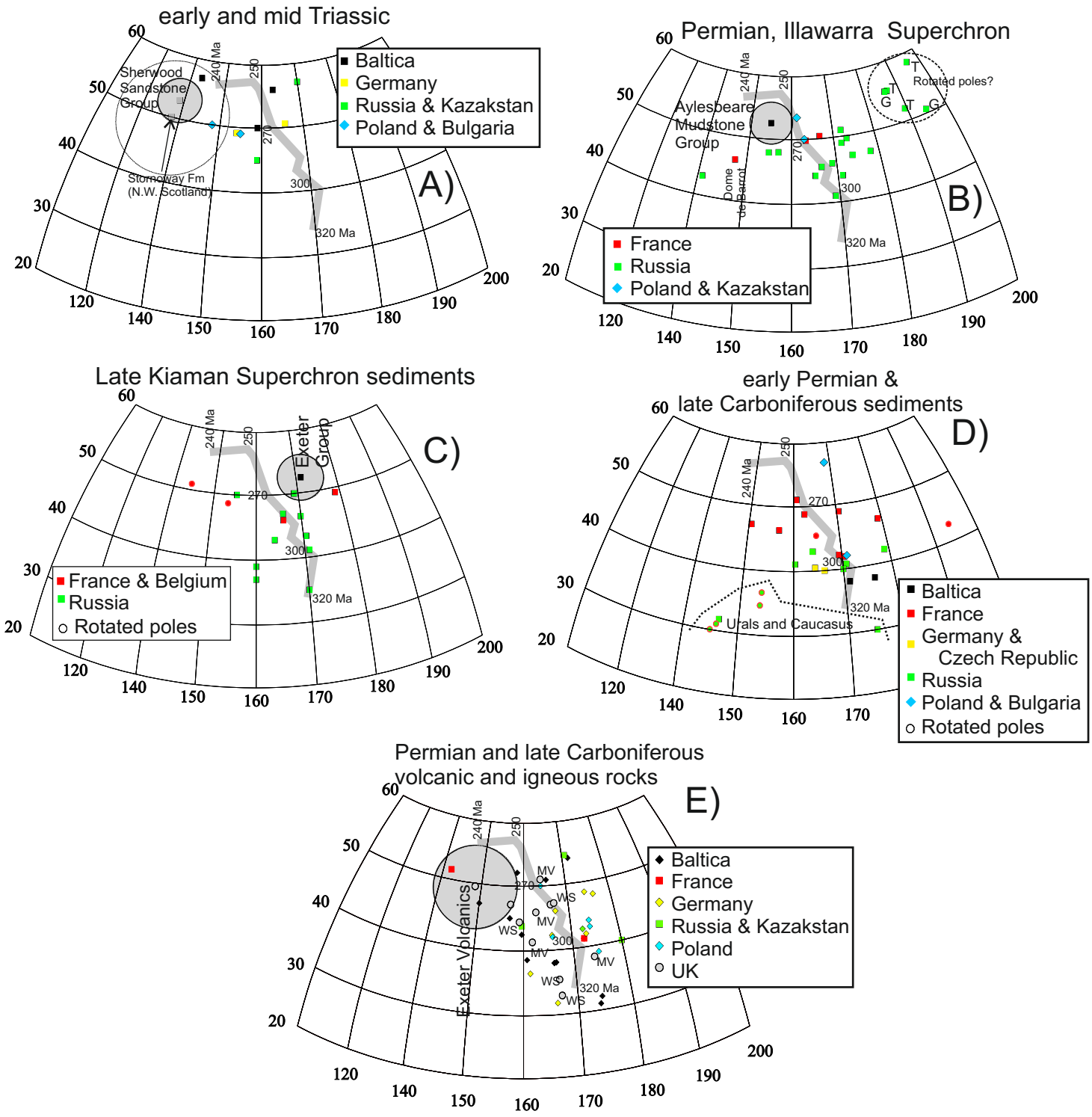

Fig. s7. Stable-Europe virtual geomagnetic poles (VGP) and their comparison to the VGP data from the latest Carboniferous, Permian and early-mid Triassic of the UK. Confidence cones for the units in SW England shown in grey, no confidence cones shown for other data. Each of the plots (A to E) shows the average European VGP path from Torsvik & Cocks (2005) labelled in Ma increments. (A) Lower and Middle Triassic sedimentary units, with Sherwood Sandstone Fm pole from Hounslow & McIntosh (2003), B) Permian sedimentary VGP data younger than the end of the KRPS (i.e. mid-late Wordian and younger). T=data from Taylor *et al.* (2009), G=from Gialanella *et al.* (1997). C) Sedimentary VGP data near the end of the KRPS. D) Lower Permian and latest Carboniferous sedimentary poles. E) Permian and latest Carboniferous volcanic and igneous-based VGP poles. MV=igneous units from the Scottish Midland Valley, WS= Whin sill data (from Liss *et al.* 2004). Data mostly from the Global Palaeomagnetic Database (http://www.ngu.no/dragon/), with newer data from Burov *et al.* (1998), Chen *et al.* (2006), Diego-Orozco *et al.* (2002), Nawrocki *et al.* (2008) and Bazhenov *et al.* (2008). In C) and D) rotated poles are filled circles.

Discussion of VGP data in Figure s7

Creer (1957), Zijderveld (1967) and Cornwall (1967) presented palaeomagnetic data for the Exeter Volcanic Rocks, around Exeter and further north in the Crediton Trough. Cornwall (1967) also performed reconnaissance sampling of the successions in this study, and from the underlying Torbay Breccia Fm. Whilst Zijderveld and Cornwall did use AF demagnetisation, and Cornwall in addition used thermal demagnetisation, relatively few of the sites measured by Cornwall (1967) had structural corrections, whereas the mean direction determined by Zijderveld utilised tilt corrections (Table 1). Cornwall's (1967) mean direction for the Exeter Volcanic Rocks has overly shallows inclination due to inclusion of some southerly-directed magnetisations with positive inclinations, probably due to incomplete demagnetisation of the specimens. The mean VGP pole of Zijderveld (1967) falls towards the end of the late Carboniferous to Permian European APWP path (Fig. s7e), which corresponds well to the range of VGP's from other late Carboniferous to Lower Permian volcanic and igneous units (Fig. S7e).

The sites from the Teignmouth Breccia and from Watcombe Cove have a significant number of specimens having declinations east of south (Table 1; Fig. 9a). The result of this is a more southerly mean, which does however, reflect new data acquired from the Russian Platform by Taylor *et al.* (2009) and Gialanella *et al.* (1997), which are clearly separated (Fig. s7b) from the bulk of previous Russian data obtained from successions younger than the Kiaman Superchron (i.e. Molostovsky 1983; Burov *et al.* 1998). Bazhenov *et al.* (2008) have discussed the problems of this new data as either due to mis-orientation, or vertical axis rotations, hitherto undetected in the eastern part of the Russian platform. Vertical axis rotations of up to 30° have also been inferred for Lower Permian sediments (Fig. s7c) in basins in France and Germany (Diego-Orozco *et al.* 2002; Chen *et al.* 2006), where there are clearer, strike-slip-related tectonic mechanisms to produce this. There are insufficient data in this study to attempt an answer to this for the UK successions, but the similarity in age and tectonic setting of these European basins, south of the Variscan Front infers a common geological or geomagnetic origin for these outlier VGP directions, warranting further investigation, beyond the scope of this study.

Supplementary Information References

Bazhenov, M.L., Grishanov, A.N., Van der Voo, R. & Levashova, N.M. 2008. Late Permian palaeomagnetic data east and west of the Urals. *Geophys. J. Int.* **173**, 395-408.

Burov, B. V., Zharkov, I. Y., Nurgaliev, D. K., Balabanov, Yu. P., Borisov, A. S. & Yasonov, P. G. 1998. Magnetostratigraphic characteristics of Upper Permian sections in the Volga and the Kama areas. In: Esaulova, N. K., Lozonsky, V. R., Rozanov, A. Yu. (eds). *Stratotypes and reference sections of the Upper Permian in the regions of the Volga and Kama Rivers*. GEOS, Moscow, 236-270.

Cornwall, J. D. 1967. Palaeomagnetism of the Exeter Lavas, Devonshire. Geophys. *Journal Royal Astro. Soc.*, **12**, 181-196.

Chen Y., Henry, B. Faure, M. ¸ Becq-Giraudon , J-F, Talbot, J-Y. Daly, L. & Le Goff, M. 2006. New Early Permian paleomagnetic results from the Brive basin (French Massif Central) and their implications for Late Variscan tectonics. *Int. J Earth Sci.*, DOI 10.1007/s00531-005-0010-5.

Creer, K. M. 1957. The Natural Remanent Magnetization of Certain Stable Rocks from Great Britain. *Philosophical Transactions of the Royal Society of London. Series A, Mathematical and Physical Sciences*, **250**, 111-129.

Diego-Orozco, A., Chen,Y., Henry, B. & Becq- Giraudond, J-F. 2002. Paleomagnetic results from the Permian Rodez basin implications: the Late Variscan tectonics in the southern French Massif Central. *Geodynamica Acta,* **15**, 249260.

Gialanella, P.R Heller, F., Haag, M. Nurgaliev, D. Borisov, A., Burov., B. Jasonov, P., Khasanov, D. Ibraginov, S. & Zharkov, I. 1997. Late Permian magnetostratigraphy on the eastern Russian Platform. *Geologie en Mijnbouw* **76**, 145-154.

Henson , M.R. 1971. *The Permo-Triassic Rocks of South Devon*. Unpublished Ph.D. Thesis, University of Exeter.

Hounslow, M.W. & McIntosh, G. 2003. Magnetostratigraphy of the Sherwood Sandstone Group (Lower and Middle Triassic): South Devon, U.K.: Detailed correlation of the marine and non-marine Anisian. *Palaeogeogr. Palaeoclimat. Palaeoecol.*, **193**, 325-348.

Jones , N.S. 1992. *Sedimentology of the Permo-Triassic of the Exeter area, S.W. England*. British Geological Survey Technical Report, WH/92/122R.

Kruiver, P. P., Dekkers, M. J. & Heslop, D. 2001. Quantification of magnetic coercivity components by the analysis of acquisition curves of isothermal remanent magnetisation. *Earth and Planetary Science Letters*, **189**, 269-276.

Laming, D. J. C. 1966. Imbrications, palaeocurrents and other sedimentary features in the Lower New Red Sandstone, Devonshire, England. *Journal of Sedimentary Petrology*, **36**, 940-959.

Liss, D., Owens, W. H. & Hutton, D. H. W. 2004. New palaeomagnetic results from the Whin Sill complex: evidence for a multiple intrusion event and revised virtual geomagnetic poles for the late Carboniferous for the British Isles. *Journal of the Geological Society, London*, **161**, 927-938.

Molostovsky, E. A. 1983. *Paleomagnetic stratigraphy of the eastern European part of the USSR*. University of Saratov, Saratov [In Russian].

Nawrocki, J. Fanning, M. Lewandowska, A., Polechoñska, O. & Werner, T. 2008. Palaeomagnetism and the age of the Cracow volcanic rocks (S Poland). *Geophys. J. Int.*, **174**, 475-488.

Selwood, E. B. Edwards, R. A., Simpson, S., Chesher, J. A. & Hamblin, R. A. 1984. *Geology of the country around Newton Abbot*. Memoir for 1:50,000 geological sheet 339, British Geological Survey, HMSO, London.

Smith, S.A. & Edwards, R.A. 1991. Regional sedimentological variations in Lower Triassic fluvial conglomerates (Budleigh Salterton Pebble Beds), southwest England: some implications for palaeogeography and basin evolution. *Geological Journal*, **26**, 65-83.

Taylor, G. K., Tucker, C., Twitchett, R. J., Kearsey, T., Benton, M. J., Newell, A. J. & Tverdokhlebov, V. P. 2009. Magnetostratigraphy of Permian/Triassic boundary sequences in the Cis-Urals, Russia: No evidence for a major temporal hiatus. *Earth and Planetary Science Letters*, **281**, 36-47.

Torsvik T. H. & Cocks L. R. M. 2005. Norway in space and time: A centennial cavalcade. Norwegian *Journal of Geology*, **85**, 73-86.

Zijderveld, J. D. A. 1967. The natural remanent magnetisation of the Exeter Volcanic Traps (Permian, Europe). *Tectonophysics*, **4**, 121-153.